

Asymptotic quasinormal frequencies of different spin fields in d -dimensional spherically-symmetric black holes

Chun-Hung Chen,^{1,*} Hing-Tong Cho,^{2,†} Anna Chrysostomou,^{3,4,‡} and Alan S. Cornell^{3,§}

¹*The Institute for Fundamental Study,
Naresuan University, Phitsanulok 65000, Thailand.*

²*Department of Physics, Tamkang University,
Tamsui District, New Taipei City, Taiwan 25137.*

³*Department of Physics, University of Johannesburg,
PO Box 524, Auckland Park 2006, South Africa.*

⁴*Université de Lyon, F-69622 Lyon, France: Université Lyon 1,
Villeurbanne CNRS/IN2P3, UMR5822,
Institut de Physique des 2 Infinis de Lyon.*

(Dated: February 9, 2022)

Abstract

While Hod’s conjecture is demonstrably restrictive, the link he observed between black hole (BH) area quantisation and the large overtone (n) limit of quasinormal frequencies (QNFs) motivated intense scrutiny of the regime, from which an improved understanding of asymptotic quasinormal frequencies (aQNFs) emerged. A further outcome was the development of the “monodromy technique”, which exploits an anti-Stokes line analysis to extract physical solutions from the complex plane. Here, we use the monodromy technique to validate extant aQNF expressions for perturbations of integer spin, and provide new results for the aQNFs of half-integer spins within higher-dimensional Schwarzschild, Reissner-Nordström, and Schwarzschild (anti-)de Sitter BH spacetimes. Bar the Schwarzschild anti-de Sitter case, the spin-1/2 aQNFs are purely imaginary; the spin-3/2 aQNFs resemble spin-1/2 aQNFs in Schwarzschild and Schwarzschild de Sitter BHs, but match the gravitational perturbations for most others. Particularly for Schwarzschild, extremal Reissner-Nordström, and several Schwarzschild de Sitter cases, the application of $n \rightarrow \infty$ generally fixes $\Re\{\omega\}$ and allows for the unbounded growth of $\Im\{\omega\}$ in fixed quantities.

PACS numbers: 04.40.b, 04.50.Gh, 04.70.s

I. INTRODUCTION

Within the highly-damped regime, the classical oscillations of a perturbed black hole (BH) known as quasinormal frequencies (QNFs) exhibit a linear, unbounded growth in the imaginary component ($\text{Im}\{\omega\}$) accompanied by a finite value for the real component ($\text{Re}\{\omega\}$) [1–30]. To first order, we can express this as

$$\lim_{n \rightarrow +\infty} \omega \sim [\text{offset}] + in [\text{gap}] , \quad (1.1)$$

where the “offset” refers to the frequency of the emitted radiation and the “gap” represents a quantised increment in the inverse relaxation time corresponding to the surface gravity.

This expression for the asymptotic quasinormal frequency (aQNF) garnered specific interest for its speculated link to a quantum theory of gravity, initiated by Hod in Ref. [31]. Motivated by Bohr’s correspondence principle and the quantised BH area spectrum proposed by Bekenstein and Mukhanov [32–34], Hod interpreted Nollert’s numerical result of

$$\text{Re}\left\{ \lim_{n \rightarrow +\infty} \omega \right\} \approx \frac{0.0437123}{M} \xrightarrow{\text{Hod}} \frac{\ln 3}{8\pi M} \quad (1.2)$$

for the Schwarzschild BH under Planck units ($c = \hbar = G = 1$) [35] as fundamental to the scaling of a “quantum Schwarzschild BH” area. Refs. [13–15, 19–21], with the application of different analytical methods, confirmed this $\ln 3/8\pi M$ result for 4D and higher-dimensional Schwarzschild BHs. On the basis of statistical arguments and the established relationships between BH entropy and surface area, Hod also derived a minimum equidistant spacing of

$$\Delta S = \ln 3 \quad (1.3)$$

for the Bekenstein-Hawking entropy spectrum. Hod considered his analysis applicable to all BHs of the Kerr-Newman “family” [31].

That classical oscillations could provide insight into quantum behaviour appeared to augur advances for a theory of quantum gravity [2–4]. Though Hod’s conjecture gained traction for several years, a possible link to a quantum theory of gravity was quickly proven tenuous when the $\ln 3$ result did not emerge for the 4D Reissner-Nordström BH in Refs. [13, 15] nor within other multi-horizon BHs inclusive or exclusive of a cosmological constant

* chun-hungc@nu.ac.th

† htcho@mail.tku.edu.tw

‡ annachrys97@gmail.com

§ acornell@uj.ac.za

[16–18, 23, 25–27, 36–40]. Furthermore, the authors of Refs. [25–27] determined that $\ln 3$ was not universal even to Schwarzschild aQNFs, as this result could only be obtained for scalar and gravitational perturbations.

Despite this, research continued into aQNFs. For example, a further iteration of Hod’s conjecture by Maggiore [29] cast BH perturbations as a collection of damped harmonic oscillations, with the real frequency defined as $\omega_0 = \sqrt{\omega_I^2 + \omega_R^2}$ and a subsequent result of

$$\Delta S = 2\pi \tag{1.4}$$

for the Bekenstein-Hawking entropy spectrum. As discussed in Refs. [4, 38], this result is more promising as it holds true for all perturbations and in a variety of BH spacetimes [41]. Interest in accessing the quantum regime through QNFs has recently led to the study of quantum corrected BHs, where only the highly-damped QNF spectra are altered; QNFs with lesser damping, in contrast, resemble the QNF spectra of classical BHs [24, 42].

Spurred initially by these early conjectured insights into quantum gravity, two comprehensive applications of analytical aQNF computational methods were produced: (i) Ref. [25], where Cho’s implementation of the modified “phase-integral” method, as put forth by Andersson and Howls [13], yielded the spin $s \in \{0, 1/2, 1, 3/2, 2\}$ QNFs in 4D Schwarzschild and Reissner-Nordström (extremal and non-extremal) BHs; (ii) Ref. [16], where Natário and Schiappa obtained aQNF expressions for gravitational perturbations in d -dimensional Minkowski and (anti-)de Sitter (AdS) BH spacetimes via the “monodromy technique” of Ref. [15]. Both methods exploit analytic continuity, with the tracing of Stokes and anti-Stokes lines to extract a physical solution from the complex plane. They differ in that the former employs a very careful “fine-structure” analysis while the latter utilises a more direct approach reliant almost exclusively on the anti-Stokes lines behaviour. These investigations motivate the present work, where we exploit the more flexible methodology used by Natário and Schiappa to extend the results of Ref. [25] to higher-dimensional Schwarzschild, Schwarzschild (A)dS, and Reissner-Nordström BH spacetimes.

To do so, we begin with a thorough review of the monodromy technique in section II. We describe the underlying principles of the method and how it is adjusted to account for BH charge and a non-zero cosmological constant. We also confirm and extend the unified treatment employed in Ref. [18] for the QNFs of Schwarzschild and Schwarzschild dS BHs: although a clear distinction is evident between the behaviour of the quasinormal mode

(QNM) potentials within the Schwarzschild “family” and Reissner-Nordström “family” of BH spacetimes near the origin, irrespective of Λ , we find that the nature of the cosmological constant dictates behaviour near spatial infinity. This observation manifests also in section III, where we study the known effective QNM potentials of various spin in order to extract the field contribution to the aQNF expressions. Finally, in section IV we demonstrate how the generalised expressions for the aQNFs and the field contributions derived in sections II and III, respectively, yield the aQNFs of the BHs of interest. Therein, we supply the new aQNFs for fields of half-integer spins within the BHs of interest. Insights, conclusions, and future directions are summarised in section V.

II. THE MONODROMY TECHNIQUE: A REVIEW

For a perfectly isolated, static, and spherically-symmetric BH of dimension $d \geq 3$, the metric function $f(r)$ is given by

$$f(r) = 1 - \frac{2\mu}{r^{d-3}} + \frac{\vartheta^2}{r^{2d-6}} - \lambda r^2, \quad (2.1)$$

which parametrises the Arnowitt-Deser-Misner (ADM) BH mass (M) and charge (Q), as well as the cosmological constant (Λ) via

$$\mu = \frac{8\pi G_d}{(d-2)\Omega_{d-2}} M, \quad \vartheta^2 = \frac{8\pi G_d}{(d-2)(d-3)} Q^2, \quad \text{and} \quad \lambda = \frac{2\Lambda}{(d-2)(d-1)},$$

respectively. G_d indicates the gravitational constant for d -dimensional spacetimes, and the area of a unit $(d-2)$ -sphere is given by Ω_{d-2} . Minkowski, dS, and AdS spacetimes are characterised by $\lambda = 0$, $\lambda > 0$, and $\lambda < 0$, respectively [43–46].

To describe the damped perturbations thereof, we can exploit the stability analyses of Refs. [43–51] which encapsulate QNM behaviour. Following the notation of Refs. [43–46], we can express the QNM in a variable-separable form,

$$\Psi(x^\mu) = \sum_{\ell, m} \frac{\Phi(r) e^{+i\omega t}}{r^{(d-2)/2}} Y_{\ell m}(\theta_i), \quad (2.2)$$

where the angular components are given by the hyper-spherical harmonics for $d-2$ angles $Y_{\ell m}(\theta_i)$, and the radial dependence may be cast into a “Schrödinger-like” ordinary differential equation,

$$\left[-\frac{d^2}{dx^2} + V[r(x)] \right] \Phi(x) = \omega^2 \Phi(x). \quad (2.3)$$

Here, $V[r(x)]$ is the effective potential, ω is the QNF, and x is the ‘‘tortoise coordinate’’ generally defined as

$$x = \int \frac{dr}{f(r)}. \quad (2.4)$$

We observe that $x = x[r]$ serves as a bijection from $(r_H, +\infty)$ to $(-\infty, +\infty)$ for asymptotically flat BH spacetimes [52], where $r = r_H$ refers to the BH event horizon. Note that in the case of dS BH spacetimes, inclusive of the cosmological horizon r_C , the bijection maps from (r_H, r_C) to $(-\infty, +\infty)$; for AdS BH spacetimes, the bijection is from $(r_H, +\infty)$ to $(-\infty, 0)$.

Near the horizon, we can express Eq. (2.4) as

$$x \sim \int \frac{dr}{(r - r_H)f'(r_H)} = \frac{1}{f'(r_H)} \log(r - r_H), \quad (2.5)$$

such that $x \rightarrow -\infty$ logarithmically when approaching r_H . For a non-degenerate horizon, with r_H as a simple zero of $f(r)$, $f'(r_H) = 2k_H$ where $k_H = 2\pi T_H$ is the surface gravity at the horizon defined in terms of the Hawking temperature T_H [16].

Near the event horizon, QNMs are purely ingoing:

$$\Phi(x) \sim e^{+i\omega x}, \quad x \rightarrow -\infty \quad (r \rightarrow r_H). \quad (2.6)$$

At spatial infinity, QNMs are purely outgoing. However, this condition manifests differently based on the nature of the cosmological constant:

$$\Phi(x) \sim \begin{cases} e^{-i\omega x}, & x \rightarrow +\infty \quad (r \rightarrow +\infty), \quad \lambda = 0, \\ e^{-i\omega x}, & x \rightarrow +\infty \quad (r \rightarrow r_C), \quad \lambda > 0, \\ 0, & x \rightarrow +\infty \quad (r \rightarrow +\infty), \quad \lambda < 0, \end{cases} \quad (2.7)$$

where r_C denotes the cosmological horizon, as before. While there are a range of possible boundary conditions applicable to AdS contexts, we remain without a convincing *a priori* argument for a universally applicable set (see Ref. [53] for discussion against an uninformed reliance on a singular set of boundary conditions in AdS BH spacetimes). Here, however, we choose to maintain Dirichlet boundary conditions near spatial infinity when considering AdS BH spacetimes, in keeping with Refs. [8, 16–18, 23, 26, 37, 38].

From the boundary conditions of Eqs. (2.6) and (2.7), the system is shown to be inherently dissipative: energy is lost at the boundaries and cannot be reintroduced. In a manner reminiscent of normal mode analyses, it is the implementation of these physically-motivated boundary conditions that discretises the QNF spectrum. The discrete QNF can then be

decomposed into its real and imaginary part, such that $\Re\{\omega\}$ represents the physical frequency of oscillation and $\Im\{\omega\}$ denotes the damping. Its dependencies include n (the “overtone” number) and ℓ (the “multipolar” or angular momentum number), the asymptotic limits of which represent regimes of interest in QNM studies. We explore the properties of QNFs subjected to $\ell \rightarrow \infty$ within Ref. [54]; here, we focus on the $n \rightarrow \infty$ regime.

As emphasised by Daghighi *et al.* in Ref. [55], “aQNFs” are those for which $|\omega| \rightarrow \infty$ while “highly damped QNFs” obey the condition $|\omega| \approx |\Im\{\omega\}| \gg |\Re\{\omega\}|$ as $n \rightarrow \infty$. This nuanced distinction becomes relevant in the computation of aQNFs within AdS spacetimes, as noted in Ref. [18] and the numerical works referenced therein, where the asymptotic limit is described as the regime in which $\Re\{\omega\} \approx \Im\{\omega\}$ [16, 18, 38]. Consequently, there exists a slight discrepancy in the decomposition of the QNF within the large overtone limit: in Minkowski and dS BH spacetimes,

$$\omega = \omega_R + in\omega_I, \quad \omega_R, \omega_I \in \mathbb{R}, \quad (2.8)$$

whereas in AdS BH spacetimes,

$$\omega = n(\omega_R + i\omega_I) + \omega_0, \quad \omega_R, \omega_I \in \mathbb{R}. \quad (2.9)$$

In setting $n \rightarrow +\infty$, ω in Eq. (2.8) for flat and dS BH spacetimes approximates to a purely imaginary number; for ω in Eq. (2.9) in AdS BH spacetimes, real and imaginary parts contribute in equally large magnitudes.

As such, the analytical calculation of the aQNF generally involves the tracing of a closed global contour from the origin to infinity in the complex r -plane, enclosing regular singular point(s). In the case of the monodromy technique, these singular points are defined by determining the complex roots of $f(r) = 0$; they represent the physical and “fictitious” [15, 16] horizons of the BH spacetime of interest. Through a comparison of the “global” monodromy computed from the contour to infinity with the “local” monodromy around the enclosed singular point(s) [19], the aQNF may be extracted.

In subsection II A, we describe the underlying requirements for this calculation and the mathematical features we exploit. Note that we adhere to the terminology utilised in Ref. [20] in our description of these contours: we consider anti-Stokes lines as lines upon which ωx is purely real (i.e. $\Im\{\omega x\} = 0$) and Stokes lines as lines upon which ωx is purely imaginary (i.e. $\Re\{\omega x\} = 0$). This is to improve comparison with the phase-integral technique, as used in Refs. [12, 22–25, 38, 55].

A. Mathematical background

The method put forth in Ref. [15] and extended in Refs. [16, 18] exploit a form of analytic continuity predicated on the fact that any solution of an ordinary differential equation can be extended from its physical region to a solution on the complex plane through the introduction of a “Wick” rotation [56]. From the effect of $n \rightarrow +\infty$ on Eqs. (2.8) and (2.9), it is clear that a continuation from the physical region $r_H < r < \infty$ to the whole complex r -plane is necessary.

To accommodate this, the boundary conditions of Eq. (2.7) undergo a transformation. For the highly-damped modes of Minkowski and dS spacetimes, the outgoing boundary conditions can be explicitly restructured as “monodromy boundary conditions” [18] consequent of the extension to the complex plane. These can be clearly stipulated: $x \sim \infty$ is “Wick rotated” to $\omega x \sim \infty$ [15, 18], such that

$$\Phi(x) \sim e^{\mp i\omega x}, \quad \begin{cases} \omega x \rightarrow \pm\infty, & \Re\{\omega\} > 0 \\ \omega x \rightarrow \mp\infty, & \Re\{\omega\} < 0. \end{cases} \quad (2.10)$$

Throughout this work, we impose $\Re\{\omega\} > 0$. For $\Re\{\omega\} < 0$, the Wick rotation is taken in the opposite direction; the method remains the same, albeit the contour drawn must be traced in the counterclockwise direction. The subsequent solution would then be the complex conjugate of that obtained under the original $\Re\{\omega\} > 0$ condition [15, 16].

The imposition of $|\omega| \rightarrow +\infty$ naturally affects Eq. (2.3): $V[r(x)]$ becomes negligible across the complex r -plane (except near singular points), such that

$$-\frac{d^2\Phi}{dx^2} \approx \omega^2\Phi(x). \quad (2.11)$$

The consequent solution is a superposition of plane waves,

$$\Phi(x) \sim A_+ e^{+i\omega x} + A_- e^{-i\omega x}. \quad (2.12)$$

Near the origin, the effective potential has been shown to retain a standard form for static and spherically-symmetric BH spacetimes, irrespective of the nature of the perturbing field [12, 15, 20, 22–25, 38, 55]:

$$V[r(x)] \Big|_{r \rightarrow 0} \sim \frac{j^2 - 1}{4x^2}, \quad (2.13)$$

where x is the complex form of the tortoise coordinate defined in Eq. (2.4). As we shall demonstrate in section III, Eq. (2.13) is achieved by defining x via Eqs. (2.14)-(2.17)

according to the BH context; in sections III and IV, we show that this j parameter is characterised by the perturbing field, and serves as the sole field contribution to the aQNF result.

Within the neighbourhood of $r \sim 0$,

$$x[r] \sim -\frac{1}{2\mu} \int dr r^{d-3} = -\frac{r^{d-2}}{2\mu(d-2)} \quad (2.14)$$

and

$$x[r] \sim \frac{1}{\vartheta^2} \int dr r^{2d-6} = \frac{r^{2d-5}}{(2d-5)\vartheta^2} \quad (2.15)$$

for the Schwarzschild and Reissner-Nordström BH “families”, respectively, regardless of the nature of the cosmological constant.

Within the region of spatial infinity ($r \sim \infty$), consistency can be found in BH spacetimes inclusive of λ rather than within a BH family. For both Schwarzschild and Reissner-Nordström BHs in asymptotically-flat spacetimes, $f(r) \sim 1$ and

$$x[r] \sim \int dr 1 = r. \quad (2.16)$$

This corresponds to a vanishing potential. For dS and AdS BH spacetimes, $f(r) \sim -\lambda r^2$ for $r \sim \infty$, such that

$$x[r] \sim \begin{cases} x_0 + \frac{1}{\lambda r} & \text{for dS } (\lambda > 0), \\ x_0 - \frac{1}{|\lambda| r} & \text{for AdS } (\lambda < 0). \end{cases} \quad (2.17)$$

The constant of integration $x_0 \in \mathbb{C}$ is introduced to ensure the choice of $x[r=0] = 0$ remains fixed, as explained in Appendix C of Ref. [16]. The corresponding potential has a form much like that of Eq. (2.13),

$$V[r(x)] \Big|_{\substack{\lambda \neq 0 \\ r \rightarrow \infty}} \sim \frac{(j^\infty)^2 - 1}{4(x - x_0)^2}, \quad (2.18)$$

where we use j^∞ to identify the parameter as distinctly associated with the singular point at $r = \infty$. This approximation of the effective potential applies for both dS and AdS BH spacetimes, as $(x - x_0)^2 \sim (\pm|\lambda|r)^{-2}$ according to Eq. (2.17).

With the approximated potentials of Eqs. (2.13) and (2.18), Eq. (2.3) within the asymptotic regions of $r \sim 0$ and $r \sim +\infty$, respectively, can then be solved through the introduction of Bessel functions of the first kind [57]. The general QNM solution becomes a linear combination of these Bessel functions,

$$\Phi(x) \sim A_+ \sqrt{2\pi\omega x} J_{+j/2}(\omega x) + A_- \sqrt{2\pi\omega x} J_{-j/2}(\omega x), \quad (2.19)$$

whose asymptotic expansions,

$$J_{\pm j/2}(\omega x) \sim \sqrt{\frac{2}{\pi\omega x}} \cos \left[\omega x - \frac{\pi}{4}(1 \pm j) \right], \quad \omega x \gg +1, \quad (2.20)$$

$$J_{\pm j/2}(\omega x) \sim \sqrt{\frac{2}{\pi\omega x}} \cos \left[\omega x + \frac{\pi}{4}(1 \pm j) \right], \quad \omega x \ll -1, \quad (2.21)$$

shall prove useful in the monodromy calculations (see subsection II C). When tracing the path along the contour, rotations can be incorporated into Bessel function solutions using a further asymptotic expansion,

$$J_{\pm j/2}(\omega x) = (\omega x)^{\pm j/2} \phi(\omega x) \Rightarrow J_{\pm j/2}(e^{i\theta}(\omega x)) = e^{\pm i\theta} e^{\pm ij/2} J_{\pm j/2}(e^{i\theta} \omega x), \quad (2.22)$$

where $\phi(\omega x)$ is considered an even holomorphic function of ωx , and $e^{i\theta} \omega x$ is real and positive [16, 24].

Within the complex r -plane, we recognise that Eq. (2.5) holds in close proximity to a specific horizon of choice. This indicates a “multi-valuedness” in the tortoise coordinate, and subsequently in the QNM solution. To avoid contending directly with this multi-valuedness, branch cuts are placed at singular points such that x “jumps” the discontinuity when $r = r_H$. We describe the corresponding behaviour of $\Phi(x)$ as it subsequently traces a closed circular path around the singular point by introducing the monodromy [15, 16].

Near the horizon, $V[r(x)] \sim 0$, which in turn leads to a plane-wave QNM solution. Thus, to determine this local monodromy for $\Phi \sim e^{\pm i\omega x}$, we consider a closed clockwise contour $\gamma \subset \mathbb{C}$ centred on $r = r_H$ (i.e. a rotation of 2π in the r -plane about the event horizon). From Eq. (2.5),

$$\begin{aligned} \log(r - r_H) &\rightarrow \log(r - r_H) - 2\pi i \\ &\Rightarrow x \sim \frac{1}{2k_H} (\log(r - r_H) - 2\pi i) \sim x - \frac{\pi i}{k_H} \\ &\Rightarrow e^{\pm i\omega x} \rightarrow e^{\pm i\omega \left(x - \frac{\pi i}{k_H} \right)} = e^{\pm i\omega x} e^{\pm \frac{\pi\omega}{k_H}}, \end{aligned}$$

which yields the local monodromy,

$$\mathfrak{M}_{\gamma, r_H}[\Phi(x)]_\ell = e^{\pm \frac{\pi\omega}{k_H}}. \quad (2.23)$$

For the global monodromy,

$$\mathfrak{M}_\gamma[\Phi(x)] = \frac{\Phi_B}{\Phi_A} \mathfrak{M}_{\gamma, r_H}[\Phi(x)]_g, \quad (2.24)$$

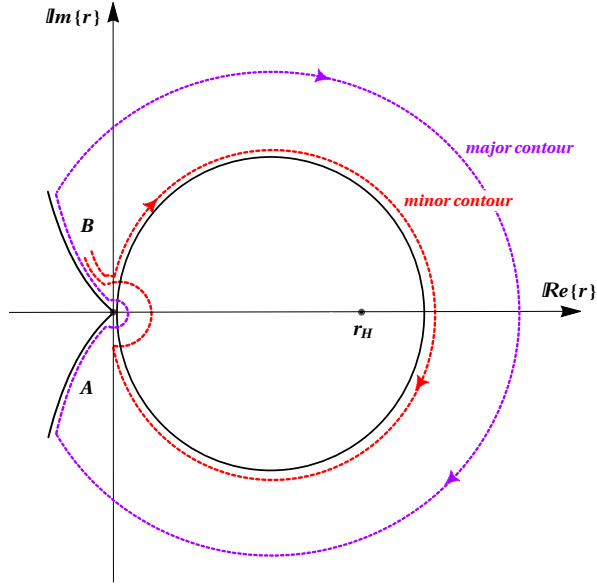


FIG. 1: *Anti-Stokes line contour within the complex r -plane for a 4D single-horizon BH. The QNM solution oscillates with neither decay nor growth along the anti-Stokes lines.*

where Φ_A and Φ_B represent the solutions on branches A and B in the complex r -plane, shown in Fig. 1 [18, 20]. The expressions for Φ_A is obtained by applying the appropriate boundary condition associated with branch A to Eq. (2.19); Φ_B is determined by incorporating the rotation Φ_A undergoes to reach branch B , and then subjecting the resultant expression to outgoing boundary conditions. Note that the monodromy at $r = +\infty$ is zero.

Since the “major” and “minor” contours include the same singular points, their monodromies are equivalent [15, 16, 18, 20]. To compute the aQNF, we equate Eqs. (2.23) and (2.24) and solve for ω .

The procedure we follow may be decomposed into two components: the set-up of the complex r -plane and the $\text{Im}\{\omega x\} = 0$ anti-Stokes lines corresponding to the BH spacetime studied (subsection II B), and the behaviour analysis of the QNM as it is traced along $\text{Im}\{\omega x\} = 0$ (subsection II C). The first component thereby contextualises the problem while the second allows for the extraction of a solution.

B. The complex r -plane set-up

With the extension of the QNM solution space for Eq. (2.3) to the complex plane comes the need to establish the positions of singular points and the path of the contour traced.

These are dictated exclusively by the BH spacetime and are independent of the perturbing field. As illustrated in Refs. [16, 18], that the aQNF in flat and dS spherically-symmetric BH spacetimes is governed by the same relationship between $\mathbb{I}m\{\omega\}$ and $\mathbb{R}e\{\omega\}$ dictates that the contour traced within the two complex r -planes must be very similar. This is shown explicitly in Figs. 5 and 6. The path traced in the AdS cases, on the other hand, differs noticeably from the flat and dS spacetimes, as exhibited in Fig. 7.

In Ref. [18], it is recommended that numerical analyses serve as aides in the construction of the contour path; in Refs. [16, 23, 38], numerical plots are used to depict the anti-Stokes lines in various dimensions. We find that we can reproduce these plots by applying the Mathematica function `ComplexPlot` to expressions of the form $-r^{d-1}/f(r)$, where $f(r)$ represents the metric function for each BH. These are sketched in Figs. 2, 3 and 4.

1. The non-AdS r -plane

To determine the position and direction of the anti-Stokes lines, we first identify the location where branch cuts shall be needed within the complex plane. This is achieved by solving for the complex roots of the metric function. For Eq. (2.1) in the dS BH spacetimes, $f(r) = 0$ produces

$$\text{Schwarzschild:} \quad -\lambda r^{d-1} + r^{d-3} - 2\mu = 0, \quad (2.25)$$

$$\text{Reissner-Nordström:} \quad -\lambda r^{2(d-2)} + r^{2(d-3)} - 2\mu r^{d-3} + \vartheta^2 = 0, \quad (2.26)$$

for which analytic solutions cannot be obtained. Thus, in order to determine the position of the horizons, roots must be calculated numerically. For even d , there are an odd and even number of roots for Schwarzschild and Reissner-Nordström BHs, respectively. These sum to zero:

$$\text{Schwarzschild:} \quad r_n = r_H, r_C, \gamma_1, \bar{\gamma}_1, \dots, \gamma_{\frac{d-4}{2}}, \bar{\gamma}_{\frac{d-4}{2}}, \tilde{r}, \quad (2.27)$$

$$\text{Reissner-Nordström:} \quad r_n = r_H^+, r_H^-, r_C, \gamma_1, \bar{\gamma}_1, \dots, \gamma_{d-4}, \bar{\gamma}_{d-4}, \tilde{r}, \quad (2.28)$$

where bars denote complex conjugates, and

$$\text{Schwarzschild:} \quad \tilde{r} = - \left[r_H + r_C + \sum_{i=1}^{\frac{d-4}{2}} (\gamma_i + \bar{\gamma}_i) \right], \quad (2.29)$$

$$\text{Reissner-Nordström:} \quad \tilde{r} = - \left[r_H^+ + r_H^- + r_C + \sum_{i=1}^{d-4} (\gamma_i + \bar{\gamma}_i) \right]. \quad (2.30)$$

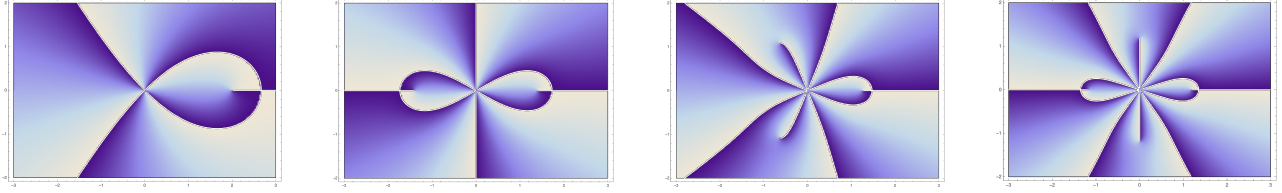
(a) $d=4$ (b) $d=5$ (c) $d=6$ (d) $d=7$

FIG. 2: Numerically generated plots illustrating the behaviour of the anti-Stokes lines for Schwarzschild BHs ($\mu = 1$).

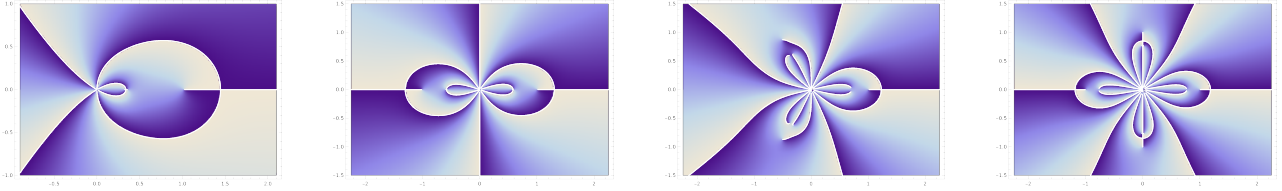
(a) $d=4$ (b) $d=5$ (c) $d=6$ (d) $d=7$

FIG. 3: Numerically generated plots illustrating the behaviour of the anti-Stokes lines for Reissner-Nordström BHs ($\mu = 1$, $\vartheta = 0.9$).

For odd d , there are an even number of roots, which sum to zero through pair-wise cancellation:

$$\text{Schwarzschild: } r_n = r_H, -r_H, r_C, -r_C, \gamma_1, \bar{\gamma}_1, \dots, \gamma_{\frac{d-5}{2}}, \bar{\gamma}_{\frac{d-5}{2}}, \quad (2.31)$$

$$\text{Reissner-Nordström: } r_n = r_H^+, r_H^-, -r_H^+, -r_H^-, r_C, -r_C, \gamma_1, \bar{\gamma}_1, \dots, \gamma_{d-5}, \bar{\gamma}_{d-5}. \quad (2.32)$$

For both even and odd d , Schwarzschild dS BHs have $(d-1)$ complex horizons, only two of which are real: the event horizon and the cosmological horizon. For Reissner-Nordström dS BHs, there are $2(d-2)$ complex horizons, with three real positive roots: the outer and inner BH horizons, as well as the cosmological horizon.

In the absence of a cosmological constant, the positions of the complex horizons become

$$\text{Schwarzschild: } r_{H_n} = \left| 2\mu \right|^{\frac{1}{d-3}} e^{\frac{2\pi i}{d-3}n}, \quad (2.33)$$

$$\text{Reissner-Nordström: } r_{H_n}^\pm = \left| \left(\mu \pm \sqrt{\mu^2 - \vartheta^2} \right)^{\frac{1}{d-3}} \right| e^{\frac{2\pi i}{d-3}n}, \quad (2.34)$$

for $n = 0, 1, \dots, d - 4$. For the Schwarzschild BH with $\lambda = 0$, there are instead $d - 3$ complex horizons, one of which is the real event horizon. The Reissner-Nordström BH has $2(d - 3)$ complex horizons and two real positive roots corresponding to the inner Cauchy horizon and outer event horizon.

In the case of the extremal Reissner-Nordström BH ($\vartheta \rightarrow \mu$), the two real horizons coalesce. The positions of the complex horizons then become

$$\text{extremal Reissner-Nordström: } r_{H_n} = |\mu|^{\frac{1}{d-3}} e^{\frac{2\pi i}{d-3}n}. \quad (2.35)$$

As observed by Andersson and Howls [13], this presents a topology distinct from both the Schwarzschild and the Reissner-Nordström BHs and therefore requires separate analysis. We shall address this further in section II C.

To draw the anti-Stokes lines around the singular points, we must adhere to the boundary conditions. As stipulated earlier, $\Im m\{\omega\} \gg \Re e\{\omega\}$ in Minkowski and dS spacetimes within the large overtone limit; since $\Im m\{\omega\} \rightarrow \infty$, the aQNF is effectively a purely imaginary quantity. Consequently, $\omega x \in \mathbb{R}$ for $x \in i\mathbb{R}$ near the origin [16]. Φ is considered to be “Wick rotated” to the anti-Stokes line of $\Im m\{\omega x\} = 0$ (which approximately corresponds to the Stokes line of $\Re e\{x\} = 0$) [15, 16, 18].

We may then establish the behaviour of the anti-Stokes lines within the neighbourhood of $r \sim 0$. From the relationship between x and r observed in Eqs. (2.14) and (2.15), we set

$$r(x) = \rho e^{i\eta(n+\frac{1}{2})}, \quad (2.36)$$

where $\rho, \eta \in \mathbb{R}$ with $\rho > 0$ as an arbitrary proportionality constant; η and n are provided in Table I [16, 18]. The above expression represents half-lines extending from the origin, spaced equally from one another by an angle of η . Since r oscillates between positive and negative values for monotonically increasing values of n , so too does the tortoise coordinate x . As such, the sign of ωx alternates between positive and negative on each subsequent half-line, anticlockwise about the origin and starting at $n = 0$ [16]. We consider the $n = 0$ line to be that which is closest to the imaginary axis in quadrant IV (see Figs. 5, 6, and 7). The branches delineating the contour emerge from the origin, superimposed onto a choice of these half-lines.

2. The AdS r -plane

As specified in Eq. (2.7), the boundary conditions for the QNMs in AdS spacetime differ from the standard form near spatial infinity. The aQNF no longer corresponds to the highly damped regime; $\Im m\{\omega\} \sim \Re e\{\omega\}$ implies that a very different anti-Stokes line topology is required. To sketch this, let us determine the positions of the complex horizons. We follow the same procedure: for Eq. (2.1) in the AdS BH spacetimes, $f(r) = 0$ produces

$$\text{Schwarzschild:} \quad |\lambda|r^{d-1} + r^{d-3} - 2\mu = 0, \quad (2.37)$$

$$\text{Reissner-Nordström:} \quad |\lambda|r^{2(d-2)} + r^{2(d-3)} - 2\mu r^{d-3} + \vartheta^2 = 0, \quad (2.38)$$

for which roots must once again be calculated numerically. For even d , there are an odd and even number of roots for Schwarzschild and Reissner-Nordström BHs, respectively. These sum to zero:

$$\text{Schwarzschild:} \quad r_n = r_H, \gamma_1, \bar{\gamma}_1, \dots, \gamma_{\frac{d-2}{2}}, \bar{\gamma}_{\frac{d-2}{2}}, \quad (2.39)$$

$$\text{Reissner-Nordström:} \quad r_n = r_H^+, r_H^-, \gamma_1, \bar{\gamma}_1, \dots, \gamma_{d-3}, \bar{\gamma}_{d-3}, \quad (2.40)$$

where our results are much like the dS cases, albeit with the absence of r_c and \tilde{r} . Similarly, for odd d , there are an even number of roots, which sum to zero through pair-wise cancellation:

$$\text{Schwarzschild:} \quad r_n = r_H, -r_H, \gamma_1, \bar{\gamma}_1, \dots, \gamma_{\frac{d-3}{2}}, \bar{\gamma}_{\frac{d-3}{2}}, \quad (2.41)$$

$$\text{Reissner-Nordström:} \quad r_n = r_H^+, r_H^-, -r_H^+, -r_H^-, \gamma_1, \bar{\gamma}_1, \dots, \gamma_{d-4}, \bar{\gamma}_{d-4}. \quad (2.42)$$

For both even and odd d , Schwarzschild AdS BHs have $(d-1)$ complex horizons, only one of which is real: the event horizon. For Reissner-Nordström AdS BHs, there are $2(d-2)$ complex horizons, with two real positive roots: the outer and inner horizons.

Near the origin, we once again set

$$r(x) = \rho e^{i\eta(n+\varphi_0)}, \quad (2.43)$$

where $\rho, \eta \in \mathbb{R}$ with $\rho > 0$ as an arbitrary proportionality constant; η and n are provided in Table I [16, 18]. As before, these half-lines extend from the origin and are spaced equally from one another by an angle of η . The sign of ωx on each of these half-lines alternates from positive to negative.

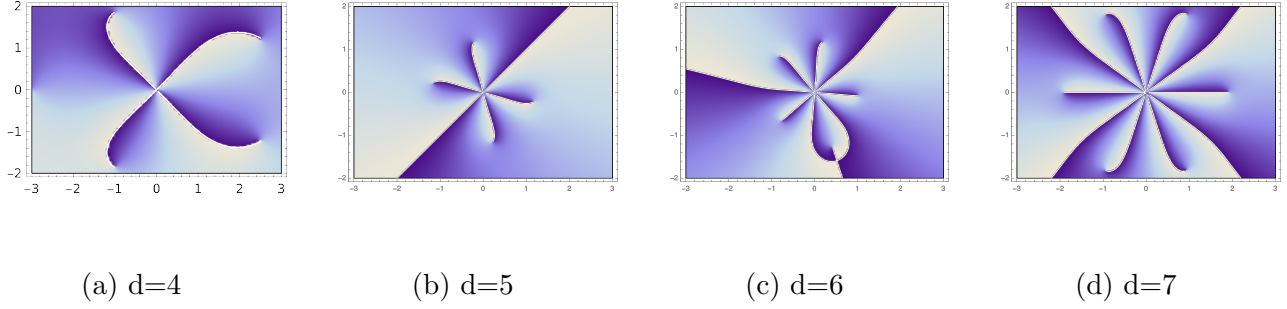


FIG. 4: Numerically generated plots illustrating the behaviour of the anti-Stokes lines for Schwarzschild AdS BHs ($\mu = \lambda = 1$).

TABLE I: Details for the sketching of the contour in the complex r -plane for flat, dS , and AdS BHs in the Schwarzschild and Reissner-Nordström (RN) “families”.

BH	η	n	branches	x for $r \sim 0$	ωx ($\lambda \geq 0$)	ωx ($\lambda < 0$)
Schwarz.	$\pi/(d-2)$	$0, 1, \dots, 2d-5$	$2(d-2)$	$-r^{d-2}/2(d-2)\mu$	$(-1)^n$	$(-1)^{n+1}$
RN	$\pi/(2d-5)$	$0, 1, \dots, 4d-11$	$2(2d-5)$	$r^{2d-5}/(2d-5)\vartheta^2$	$(-1)^{n+1}$	$(-1)^n$

However, $\Im m\{\omega x\}$ remains multi-valued around all horizons, such that a particular branch must be chosen from which we trace the $\Im m\{\omega x\} = 0$ line. The need for a shifting of the branch cuts emerges to ensure that $\Im m\{\omega x\} = 0$ does not intersect with the complex horizons established for the AdS BHs. Since at least one branch must extend to spatial infinity, we can select branch cuts in such a way that a branch in quadrant I must correspond to $r \sim \infty$. From Eq. (2.17),

$$\omega x \sim \omega x_0 - \omega \frac{1}{|\lambda|r} \quad (2.44)$$

for $r \sim \infty$. Since $\Im m\{\omega\} \sim \Re e\{\omega\}$ for aQNFs in AdS spacetimes, ωx_0 is approximately real in the asymptotic limit. Consequently, we may claim that $\arg\{\omega\} = -\arg\{x_0\} \equiv -\varphi_0$ [16]. The argument of r along the branch extending towards spatial infinity is then equivalent to $-\varphi_0$. The contour informed by these considerations is demonstrated in Fig. 7.

C. The aQNF calculation

While their explicit monodromy calculations are based on contours traced for 6D BH spacetimes, the final gravitational aQNF expressions computed by Natário and Schiappa in Ref. [16] are claimed to be applicable for spacetimes of dimension $d > 3$. Such generalisability of $d = 6$ spin-2 aQNF results has also been alluded to in Refs. [23, 38]. Since we find that generalised aQNF expressions can be calculated without consideration of the nature of the perturbing field, these claims of universal applicability for $d > 3$ may be extended to the results presented throughout this section.

1. Schwarzschild and Schwarzschild dS BHs

In Fig. 5, the contour drawn remains identical for Schwarzschild and Schwarzschild dS BHs – only the “contents” enclosed by the contour and the behaviour of the QNM near spatial infinity differ. As such, the solutions on the major contour can be traced uniformly for Schwarzschild and Schwarzschild dS BHs, as first stipulated in Ref. [18].

We begin the path on branch A . Near the origin, we know the potential has the standard form depicted in Eq. (2.13). The positive ωx of the $n = 0$ branch implies that we can exploit the asymptotic expansion of the Bessel function associated with $\omega x \gg 1$, such that

$$\begin{aligned} \Phi(x) &\sim B_+ \sqrt{2\pi\omega x} J_{+j/2}(\omega x) + B_- \sqrt{2\pi\omega x} J_{-j/2}(\omega x) \\ &\sim (B_+ e^{-i\alpha_+} + B_- e^{-i\alpha_-}) e^{+i\omega x} + (B_+ e^{+i\alpha_+} + B_- e^{+i\alpha_-}) e^{-i\omega x}. \end{aligned} \quad (2.45)$$

Furthermore, the appropriate boundary condition on A is purely outgoing, *viz.*

$$\begin{aligned} \omega x \rightarrow +\infty &\Rightarrow \Phi \sim e^{-i\omega x} \\ &\Rightarrow B_+ e^{-i\alpha_+} + B_- e^{-i\alpha_-} = 0. \end{aligned} \quad (2.46)$$

Consequently, the solution on branch A is

$$\Phi_A(x) \sim (B_+ e^{+i\alpha_+} + B_- e^{+i\alpha_-}) e^{-i\omega x}. \quad (2.47)$$

To reach branch B , a rotation of 3η in r (corresponding to 3π in x) is needed. We invoke Eq. (2.22) to incorporate the rotation into the general solution of Eq. (2.19). To simplify, we utilise the exponential form of $\cos x \equiv (e^{+ix} + e^{-ix})/2$ and $e^{3\pi i} = -1$; we also define $\alpha_{\pm} \equiv (1 \pm j)\pi/4$:

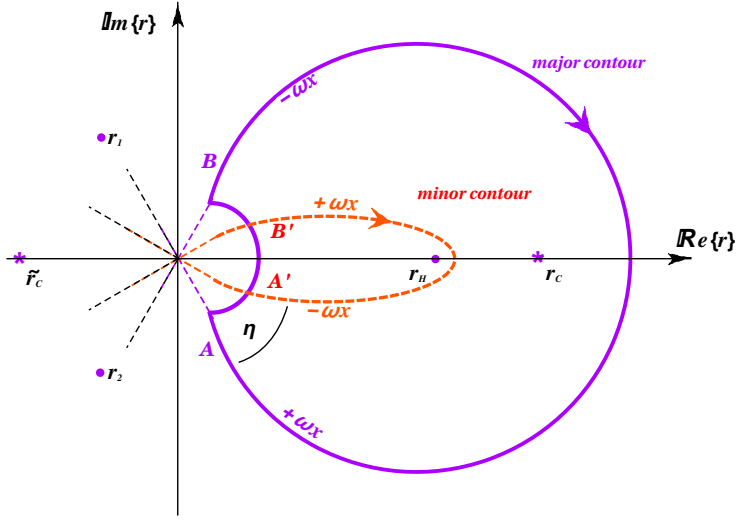


FIG. 5: Anti-Stokes lines for a Schwarzschild dS BH with $d = 6$.

For $\lambda > 0$, $r_i \rightarrow \gamma_i$ and r_c, \tilde{r}_c remain.

$$\begin{aligned}
\Phi(x) &\sim B_+ \sqrt{2\pi e^{3\pi i} \omega x} J_{+j/2}(e^{3\pi i} \omega x) + B_- \sqrt{2\pi e^{3\pi i} \omega x} J_{-j/2}(e^{3\pi i} \omega x) \\
&\sim B_+ 2 \cos(-\omega x - \alpha_+) e^{6i\alpha_+} + B_- 2 \cos(-\omega x - \alpha_-) e^{6i\alpha_-} \\
&= (B_+ e^{7i\alpha_+} + B_- e^{7i\alpha_-}) e^{+i\omega x} + (B_+ e^{5i\alpha_+} + B_- e^{5i\alpha_-}) e^{-i\omega x}. \tag{2.48}
\end{aligned}$$

Though $\omega x < 0$ on branch B , the fact that the path is traced towards infinity requires that we maintain the use of outgoing boundary conditions. Thus,

$$\begin{aligned}
\omega x \rightarrow +\infty &\Rightarrow \Phi \sim e^{-i\omega x} \\
&\Rightarrow B_+ e^{7i\alpha_+} + B_- e^{7i\alpha_-} = 0, \tag{2.49}
\end{aligned}$$

such that the general solution at branch B becomes

$$\Phi_B(x) \sim (B_+ e^{5i\alpha_+} + B_- e^{5i\alpha_-}) e^{-i\omega x}. \tag{2.50}$$

For the higher-dimensional Schwarzschild BH, the computation of the local and global monodromies directly follows the discussion outlined in subsection II A. The former requires a clockwise path governed by the ingoing boundary conditions, such that $\Phi \sim e^{+i\omega x}$. Along the path, x increases by $-2\pi i/2k_H$, such that the local monodromy is given by

$$\mathfrak{M}_{\gamma, r_H}[\Phi(x)] = e^{+\frac{\pi\omega}{k_H}}. \tag{2.51}$$

The global monodromy associated with the major contour of Fig. 5 traced to spatial infinity adheres to the outgoing boundary conditions, such that $\Phi \sim e^{-i\omega x}$. We therefore require the coefficients of $e^{-i\omega x}$ from Eqs. (2.45) and (2.48), as well as the clockwise monodromy of $e^{-i\omega x}$. Since x also increases by $-2\pi i/2k_H$ on this path, the result is $e^{-\pi\omega/k_H}$. Thus, the global monodromy becomes

$$\mathfrak{M}_\gamma[\Phi(x)] = \frac{B_+ e^{5i\alpha_+} + B_- e^{5i\alpha_-}}{B_+ e^{+i\alpha_+} + B_- e^{+i\alpha_-}} e^{-\frac{\pi\omega}{k_H}}. \quad (2.52)$$

To obtain the final expression for the aQNF within the Schwarzschild BH, we equate the monodromies and solve

$$\frac{B_+ e^{5i\alpha_+} + B_- e^{5i\alpha_-}}{B_+ e^{+i\alpha_+} + B_- e^{+i\alpha_-}} e^{-\frac{\pi\omega}{k_H}} = e^{+\frac{\pi\omega}{k_H}}. \quad (2.53)$$

The aQNF solution is obtained by writing Eq. (2.53) and the additional boundary condition of Eq. (2.46) as a system of linear equations in matrix form $X(B_+, B_-)^T = 0$, and then solving for $\det(X) = 0$. This procedure applies to all spacetimes studied in this work. However, for the Schwarzschild BH family, we solve for the aQNF using the derivative of the determinant $\partial_j \det(X) = 0$ instead [16].

We can generalise the solution provided in Ref. [16] for the aQNF within the Schwarzschild BH spacetimes, such that

$$\lim_{n \rightarrow \infty} \omega = T_H \ln(-1 - 2 \cos(\pi j)) + 2\pi i T_H n, \quad (2.54)$$

where $T_H = k_H/2\pi$. This is in agreement with Refs. [9, 15, 19], and is in keeping with the aQNF “structure” given in Eq. (1.1) for the highly-damped QNFs of the 4D Schwarzschild BH.

For the d -dimensional Schwarzschild dS BH, these considerations are augmented by the presence of the cosmological horizon at $r = r_c$, where $r_H \ll r_c$. We find that this leads to the establishment of two global monodromy expressions: an adapted Eq. (2.52) incorporating the surface gravity at $r = r_c$ ($k_c < 0$) where outgoing boundary conditions dominate the overall behaviour ($\Phi \sim e^{-i\omega x}$), and a second expression where ingoing boundary conditions dominate ($\Phi \sim e^{+i\omega x}$). Thus two “monodromy equations” emerge that must be solved simultaneously to extract the aQNF.

Let us begin with the local monodromies. Around r_c , we trace a clockwise path governed by the outgoing boundary conditions, such that $\Phi \sim e^{-i\omega x}$, along which x increases by

$-2\pi i/2k_C$. Thus, the local monodromy associated with r_C is

$$\mathfrak{M}_{\gamma, r_C}[\Phi(x)] = e^{-\frac{\pi\omega}{k_C}}. \quad (2.55)$$

Eq. (2.51) remains valid, such that the tightly wound contour around the regular singular points yields a local monodromy of

$$\mathfrak{M}_{\gamma, r_i}[\Phi(x)] = e^{+\frac{\pi\omega}{r_H} - \frac{\pi\omega}{k_C}}. \quad (2.56)$$

The first global monodromy is obtained from Eq. (2.52), where we now include the increase of $-2\pi i/2k_C$ in x under the influence of outgoing boundary conditions. Thus,

$$\mathfrak{M}_{\gamma}[\Phi(x) \sim e^{-i\omega x}] = \frac{B_+ e^{5i\alpha_+} + B_- e^{5i\alpha_-}}{B_+ e^{+i\alpha_+} + B_- e^{+i\alpha_-}} e^{-\frac{\pi\omega}{k_H} - \frac{\pi\omega}{k_C}}. \quad (2.57)$$

For the second global monodromy, we apply ingoing boundary conditions to Eqs. (2.45) and (2.48) in order to extract the $e^{+i\omega x}$ terms. Since the increase in x by $2\pi i/2k_i$ yields $e^{+i\omega(-\pi i/k_H)} e^{+i\omega(-\pi i/k_C)}$, the second global monodromy becomes

$$\mathfrak{M}_{\gamma}[\Phi(x) \sim e^{+i\omega x}] = \frac{B_+ e^{7i\alpha_+} + B_- e^{7i\alpha_-}}{B_+ e^{-i\alpha_+} + B_- e^{-i\alpha_-}} e^{+\frac{\pi\omega}{k_H} + \frac{\pi\omega}{k_C}}. \quad (2.58)$$

In solving the two simultaneous equations

$$\frac{B_+ e^{5i\alpha_+} + B_- e^{5i\alpha_-}}{B_+ e^{+i\alpha_+} + B_- e^{+i\alpha_-}} e^{-\frac{\pi\omega}{k_H} - \frac{\pi\omega}{k_C}} = e^{+\frac{\pi\omega}{r_H} - \frac{\pi\omega}{k_C}}, \quad (2.59)$$

$$\frac{B_+ e^{7i\alpha_+} + B_- e^{7i\alpha_-}}{B_+ e^{-i\alpha_+} + B_- e^{-i\alpha_-}} e^{+\frac{\pi\omega}{k_H} + \frac{\pi\omega}{k_C}} = e^{+\frac{\pi\omega}{r_H} - \frac{\pi\omega}{k_C}}, \quad (2.60)$$

we may extract a fully generalised solution for the aQNF,

$$\left(-3e^{\pi ij + 2\left(\frac{\pi\omega}{k_C} + \frac{\pi\omega}{k_H}\right)} + 3e^{2\pi ij + 2\left(\frac{\pi\omega}{k_C} + \frac{\pi\omega}{k_H}\right)} + e^{\pi ij + \frac{2\pi\omega}{k_C}} + e^{\pi ij + \frac{2\pi\omega}{k_H}} - 3e^{\pi ij} + 3e^{2\pi ij} + 3e^{2\left(\frac{\pi\omega}{k_C} + \frac{\pi\omega}{k_H}\right)} + 3 \right) \times (1 + e^{\pi ij}) e^{-\frac{3}{2}\pi ij - \left(\frac{\pi\omega}{k_C} + \frac{\pi\omega}{k_H}\right)} = 0. \quad (2.61)$$

This can be shown to be in agreement with Refs. [16, 26, 37]. As demonstrated in Ref. [26], the aQNF solution can instead be extracted in trigonometric form, such that

$$\sin\left(\frac{3\pi}{2}j\right) \cosh\left(\frac{\pi\omega}{k_C} + \frac{\pi\omega}{k_H}\right) + \sin\left(\frac{\pi}{2}j\right) \cosh\left(\frac{\pi\omega}{k_H} - \frac{\pi\omega}{k_C}\right) = 0. \quad (2.62)$$

If differentiated with respect to j and then subjected to $j \rightarrow 0$, Eq. (2.62) reduces to the Schwarzschild dS aQNF given in Ref. [16].

Within the investigations of Refs. [16, 26], it was noted that the Schwarzschild dS aQNF reduces to the aQNF of the Schwarzschild BH. To demonstrate this, we exploit the fact that $r_C \sim \lambda^{-1/2}$ [38]. Since the Schwarzschild BH spacetime does not possess a cosmological horizon, we set $\lambda \rightarrow 0^+$ such that $r_C \rightarrow +\infty$. Consequently,

$$k_C = \frac{1}{2}f'(r_C) \sim -\lambda r_C \sim -\frac{1}{r_C} \quad \Rightarrow \quad k_C \sim 0^+. \quad (2.63)$$

For gravitational perturbations, where $j = 0, 2$ depending on the mode studied, Eq. (2.61) was shown in Ref. [16] to reduce to

$$e^{\frac{\pi\omega}{k_H}} + 3e^{-\frac{\pi\omega}{k_H}} = 0 \quad \Rightarrow \quad e^{\frac{2\pi\omega}{r_H}} = -3. \quad (2.64)$$

This leads precisely to the expression for the gravitational aQNFs of a Schwarzschild BH [15, 16, 19], which we may obtain from Eq. (2.54) with the appropriate values of j .

A further remark from the studies of Refs. [16, 26, 37] concerns the anomalies associated with the $d = 4$ and $d = 5$ Schwarzschild dS BHs, based on the manner in which the contours are drawn (please see Fig. 2 for comparison, and recall the similarity between Schwarzschild and Schwarzschild dS BH contours). In the case of the 4D Schwarzschild dS BH, the anticlockwise monodromy at \tilde{r}_C must be taken into account, in conjunction with the clockwise monodromy around r_H and r_C . The first monodromy, however, is equivalent to the latter two, and the final expression for the aQNF is exactly that of Eq. (2.61). Since the $d = 4$ contour can be deformed into its $d = 6$ counterpart [16], such a result is to be expected.

For the 5D Schwarzschild dS BH, the anti-Stokes line closes near spatial infinity. The solution in this region was provided in Eq. (2.18), and serves as the QNM expression at point B . In Ref. [16], tensor-, vector-, and scalar-modes were observed to correspond to $j^\infty = 4, 2, 0$, respectively. To move from branch B to A , a rotation of $\pi/2$ must be introduced, which in turn produces

$$\Phi(x) \sim (C_+ e^{3i\beta_+} + C_- e^{3i\beta_-}) e^{+i\omega(x-x_0)} + (C_+ e^{+i\beta_+} + C_- e^{+i\beta_-}) e^{-i\omega(x-x_0)}. \quad (2.65)$$

With these corrections made, the calculation follows the method outlined above, and yields the aQNF solution

$$\sin\left(\frac{3\pi}{2}j\right) \sinh\left(\frac{\pi\omega}{k_H} + \frac{\pi\omega}{k_C}\right) - \sin\left(\frac{\pi}{2}j\right) \sinh\left(\frac{\pi\omega}{k_H} - \frac{\pi\omega}{k_C}\right) = 0, \quad (2.66)$$

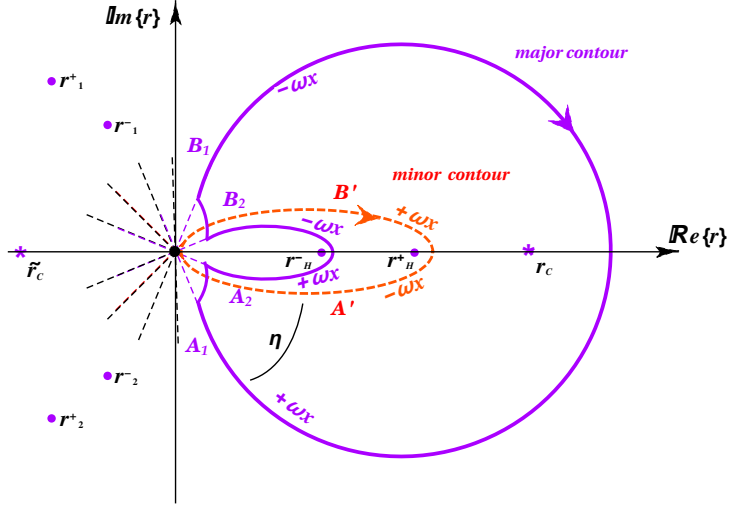


FIG. 6: *Anti-Stokes lines for a Reissner-Nordström dS BH with $d = 6$.*

If we set $\lambda = 0$, r_c and \tilde{r}_c vanish.

as shown in Ref. [26]. Once again, differentiating with respect to j and then applying $j \rightarrow 0$ produces the corresponding result given in Ref. [16]. These, too, reduce to the Schwarzschild solution within the $r_c \rightarrow +\infty$ limit.

2. Reissner-Nordström and extremal Reissner-Nordström BHs

In Fig. 6, the shape of the major contour is shown to include a rotation from A_1 to A_2 , a loop around the inner horizon, and a further rotation from B_2 to B_1 . We define the change in x due to this rotation about the Cauchy horizon as δ .

Let us begin with the Reissner-Nordström BH spacetime, within the neighbourhood of the origin. On branch A_1 , $\omega x \gg 1$. As in the Schwarzschild case, the purely outgoing boundary condition is applied; the general solution of Eq. (2.45) at A_1 becomes

$$\Phi_{A_1}(x) \sim (B_+ e^{+i\alpha_+} + B_- e^{+i\alpha_-}) e^{-i\omega x}, \quad (2.67)$$

and a boundary condition of

$$B_+ e^{-i\alpha_+} + B_- e^{-i\alpha_-} = 0 \quad (2.68)$$

emerges.

A rotation of 2η in r , or 2π in x , is needed to reach branch A_2 , where Eq. (2.20) applies. We invoke Eq. (2.22) to incorporate the rotation into the solution of Eq. (2.19), and exploit

$e^{2\pi i} = +1$:

$$\Phi_{A_2}(x) \sim (B_+ e^{3i\alpha_+} + B_- e^{3i\alpha_-}) e^{+i\omega x} + (B_+ e^{5i\alpha_+} + B_- e^{5i\alpha_-}) e^{-i\omega x} . \quad (2.69)$$

We now encounter the loop around $r = r_H^-$. The path from A_2 to B_2 is anticlockwise, such that x increases by $\delta = +2\pi i/2k_H^-$. Note that on branch B_2 , $\omega x < 0$, such that we expand the Bessel functions according to Eq. (2.21). The general QNM solution therefore becomes

$$\Phi_{B_2}(x) \sim (C_+ e^{i(\alpha_+ - \omega\delta)} + C_- e^{i(\alpha_- - \omega\delta)}) e^{i\omega x} + (C_+ e^{-i(\alpha_+ - \omega\delta)} + C_- e^{-i(\alpha_- - \omega\delta)}) e^{-i\omega x} . \quad (2.70)$$

We match the solutions of Eqs. (2.69) and (2.70) by equating their coefficients of $e^{\pm i\omega x}$:

$$B_+ e^{3i\alpha_+} + B_- e^{3i\alpha_-} = C_+ e^{i(\alpha_+ - \omega\delta)} + C_- e^{i(\alpha_- - \omega\delta)} , \quad (2.71)$$

$$B_+ e^{5i\alpha_+} + B_- e^{5i\alpha_-} = C_+ e^{-i(\alpha_+ - \omega\delta)} + C_- e^{-i(\alpha_- - \omega\delta)} . \quad (2.72)$$

To rotate from B_2 to B_1 , we require a further rotation in r of 2η (i.e. 2π in $(x - \delta)$); with $e^{2\pi i} = +1$, this introduces no change. On branch B_1 , $\omega x < 0$, such that Eq. (2.21) applies and the QNM solution becomes

$$\Phi_{B_1}(x) \sim (C_+ e^{5i\alpha_+} + C_- e^{5i\alpha_-}) e^{+i\omega(x-\delta)} + (C_+ e^{3i\alpha_+} + C_- e^{3i\alpha_-}) e^{-i\omega(x-\delta)} . \quad (2.73)$$

For the global and local monodromies, only the outer horizon is taken into account. For the latter, x increases by $-2\pi i/k_H^+$ along the clockwise path of $\Phi \sim e^{+i\omega x}$, such that

$$\mathfrak{M}_{\gamma, r_H^+}[\Phi(x)] = e^{+\frac{\pi\omega}{k_H^+}} \quad (2.74)$$

is the local monodromy. Since the global monodromy is associated with the path to spatial infinity, the $e^{-i\omega x}$ coefficients of Eqs. (2.45) and (2.73) combine with $e^{-i\omega(\pi i/k_H^+)}$ to produce

$$\mathfrak{M}_{\gamma}[\Phi(x)] = \frac{(C_+ e^{3i\alpha_+} + C_- e^{3i\alpha_-}) e^{+i\omega\delta}}{B_+ e^{+i\alpha_+} + B_- e^{+i\alpha_-}} e^{-\frac{\pi\omega}{k_H^+}} . \quad (2.75)$$

With the aid of the boundary conditions introduced in Eqs. (2.68), (2.71), and (2.72), the aQNF can be extracted from

$$\frac{(C_+ e^{3i\alpha_+} + C_- e^{3i\alpha_-}) e^{+i\omega\delta}}{B_+ e^{+i\alpha_+} + B_- e^{+i\alpha_-}} e^{-\frac{\pi\omega}{k_H^+}} = e^{+\frac{\pi\omega}{k_H^+}} \quad (2.76)$$

$$\Rightarrow e^{\frac{2\pi\omega}{k_H^+}} = -(1 + 2 \cos(\pi j)) - (2 + 2 \cos(\pi j)) e^{-\frac{2\pi\omega}{k_H^+}} . \quad (2.77)$$

Confirmation of this aQNF solution can be found in Refs. [13, 15, 58].

The Reissner-Nordström metric lends itself naturally to assessment within different limits. Let us first consider $\vartheta \rightarrow 0$: since the metric reduces to that of the Schwarzschild form under this condition, the Cauchy horizon at $r = r_H^-$ vanishes and only the outer horizon at $r = r_H^+$ remains. The surface gravity defined as $k_H^\pm = 1/2f'(r_H^\pm)$ at each horizon then becomes

$$k_H^- \sim -\frac{(d-3)\mu}{(r_H^-)^{d-2}} \rightarrow -\infty \quad \text{and} \quad k_H^+ \sim \frac{(d-3)\mu}{(r_H^+)^{d-2}}, \quad (2.78)$$

respectively. Consequently, $e^{-2\pi\omega/k_H^-} \rightarrow 1$, and Eq. (2.77) reduces to

$$e^{+\frac{2\pi\omega}{k_H^+}} = -(3 + 4\cos(\pi j)) . \quad (2.79)$$

As such, we see that although the Reissner-Nordström BH metric resembles the Schwarzschild BH metric in the $\vartheta \rightarrow 0$ limit, the expression corresponding to the aQNF does not follow suit.

This issue was first addressed in Ref. [13]. There, the real part of the aQNF of the 4D Reissner-Nordström BH reduced to $\ln 5$ when $Q \rightarrow 0$, in contradiction to the $\ln 3$ of the 4D Schwarzschild BH for which $Q = 0$. To explain this, Andersson and Howls suggested that two separate scales correspond to the Reissner-Nordström BH problem, demarcated by the non-commuting limits $|\omega| \approx |\omega_I| \rightarrow \infty$ and $Q \rightarrow 0$. Applying the former first yields $\ln 5$; applying the latter first yields $\ln 3$. While Andersson and Howls confirm that $\ln 5$ represents the correct expression for the highly-damped aQNFs of the 4D Reissner-Nordström BH, they consider the existence of an “intermediate” damping range for which $\Re\{\omega\} \approx \ln 3$ within the Reissner-Nordström BH spacetime. By order of magnitude estimates for $d = 4$, Refs. [13, 22, 24] define this range in terms of Newton’s gravitational constant and the ADM mass:

$$1 \ll (GM)|\omega| \ll \left(\frac{GM}{Q}\right)^4 . \quad (2.80)$$

Of greater interest is the $\vartheta \rightarrow \mu$ limit that characterises the extremal Reissner-Nordström BH. While it is known that the unique topology of this extremal case requires its own individual analytical treatment [13, 16, 17, 23, 25], there is contention within the literature on the correct way to perform such an analysis. One example lies in Ref. [17], where interpretation of the anti-Stokes line behaviour at the origin (specifically, a rotation of π in the 4D complex plane rather than the expected $5\pi/3$) has been criticised by the authors of Refs. [16, 23, 38]. However, we see this inconsistency in the treatment of the extremal BH

more clearly when comparing the results of Ref. [16] and [23]. The former produced the aQNF expression for the extremal Reissner-Nordström BH

$$e^{\frac{2\pi\omega}{k}} = \frac{\sin\left(\frac{5\pi j}{2}\right)}{\sin\left(\frac{\pi j}{2}\right)} \quad (2.81)$$

through an application of the monodromy technique utilised throughout this work. The latter applied the more involved phase-integral method and obtained an expression of the form

$$e^{\frac{2\pi\omega}{k}} = -(2 + 2\cos(\pi j)) \quad (2.82)$$

To our knowledge, this is the only known example where the two analytical techniques produce different results for the aQNF expression. If we compare Fig. 5 of Ref. [16] and Fig. 1 of Ref. [23], it is clear that both groups used the correct BH topology. However, while tracing the contour around the event horizon, the authors of Ref. [16] crossed two anti-Stokes lines connected to the horizon without applying the QNM boundary conditions, which in turn led to an incorrect monodromy. This may invalidate Eq. (2.81). The more reliable result seems to be that of Eq. (2.82); subsequent discussion on the aQNFs of the extremal Reissner-Nordström BH shall be based on this result.

Further validation of the Eq. (2.82) is outstanding. We believe this strongly motivates for additional focus on the aQNFs of the extremal Reissner-Nordström BH through numerical approaches, which have been sparse to date. Difficulty in producing a stable numerical method for the computation of the aQNFs of extremal Reissner-Nordström BHs has also been encountered, as seen in Ref. [10]. In Ref. [59], the authors stated that the direct application of Leaver's continued fraction method – known to be a reliable means by which to calculate aQNFs – fails in the case of the extremal Reissner-Nordström BH. Through a change in variable introduced by Onozawa *et al.* [60], the problem can be reduced to a five-term recurrence relation [59].

We note with interest that Eq. (2.82) is the result determined in Ref. [16] when $\vartheta \rightarrow \mu$ is applied to Eq. (2.77). Although $\vartheta \rightarrow \mu$ and $n \rightarrow \infty$ are also a set of non-commuting limits (just like $\vartheta \rightarrow 0$ and $n \rightarrow \infty$), the extremal limit of the aQNF of the non-extremal Reissner-Nordström BH from Ref. [16] agrees with the extremal limit of the aQNF for the extremal Reissner-Nordström BH calculated in Ref. [23]. We consider this to be a coincidence.

In both Eqs. (2.81) and (2.82), we utilise a parameter k instead of the surface gravity

k_H , where

$$k = \frac{1}{2} f'(r_H) = \frac{1}{2} \frac{(d-3)^2}{(d-2)\mu^{\frac{1}{d-3}}}. \quad (2.83)$$

As mentioned in section I, surface gravity is well-defined only for non-extremal BHs; Hawking radiation is therefore not associated with extremal BHs. However, we can define an analogous function $T = k/2\pi$ [16] where

$$T = \frac{d-3}{d-2} \left(\frac{d-3}{4\pi\mu^{\frac{1}{d-3}}} \right). \quad (2.84)$$

Moreover, for certain values of j , the real part of the aQNF includes the natural logarithm of an integer. Though provocative, Hod's conjecture cannot apply here: its underlying arguments [32, 33, 61] are restricted to non-extremal cases, thereby rendering Hod's argument invalid. Moreover, we must recognise that proof of the stability of perturbing fields within the extremal Reissner-Nordström BH spacetime is still outstanding (see section VIII of Ref. [4]), which implies any results within the extremal Reissner-Nordström BH context must be approached with some scrutiny. Despite this, the extremal Reissner-Nordström case remains a fascinating BH spacetime with extensive applications ranging from numerical development (see Ref. [54] and references therein) to supersymmetry (SUSY) considerations [62, 63], the latter of which shall be addressed in section IV.

3. Schwarzschild AdS BHs

For static and spherically-symmetric AdS BHs, the absence of a closed contour implies that monodromy considerations cannot be incorporated. Consequently, for the Schwarzschild AdS BH Natário and Schiappa's approach becomes a simple matter of matching solutions across the path traced in Fig. 7.

We begin in the region near spatial infinity, on branch B . The form of the potential is given in Eq. (2.18); the corresponding solution is of the form of Eq. (2.19). Since $\omega x < 0$ on this branch, we apply the asymptotic expansion of Eq. (2.21). However, the vanishing energy flux boundary conditions we employ in this work nullify the C_- term. Thus,

$$\Phi_{B_{r \sim \infty}}(x) \sim C_+ e^{+i\beta_+} e^{+i\omega(x-x_0)} + C_+ e^{-i\beta_+} e^{-i\omega(x-x_0)}, \quad (2.85)$$

where we introduce $\beta_+ = (1 + j^\infty) \pi/4$.

The path is traced from spatial infinity to the neighbourhood of the origin. The potential for $r \sim 0$, Eq. (2.13), yields a QNM solution of the form of Eq. (2.19), which decomposes under Eq. (2.21) to

$$\Phi_{B_{r \sim 0}}(x) \sim (B_+ e^{-i\alpha_+} + B_- e^{-i\alpha_-}) e^{i\omega x} + (B_+ e^{i\alpha_+} + B_- e^{i\alpha_-}) e^{-i\omega x}. \quad (2.86)$$

We equate the coefficients of $e^{\pm i\omega x}$ from Eqs. (2.85) and (2.86). These resultant expressions should also be equivalent, such that

$$(B_+ e^{-i\alpha_+} + B_- e^{-i\alpha_-}) e^{-i\beta_+} e^{+i\omega x_0} = (B_+ e^{i\alpha_+} + B_- e^{i\alpha_-}) e^{+i\beta_+} e^{-i\omega x_0} \quad (2.87)$$

serves as a boundary condition for the aQNF calculation.

To move from branch B to A , the rotation in r is through $-\eta$ (i.e. $-\pi$ in x). Since $e^{-i\pi} = -1$ and $\omega x > 0$ on branch A , Eq. (2.20) applies and the general solution on branch A becomes

$$\Phi_A(x) \sim (B_+ e^{-i\alpha_+} + B_- e^{-i\alpha_-}) e^{+i\omega x} + (B_+ e^{-3i\alpha_+} + B_- e^{-3i\alpha_-}) e^{-i\omega x}. \quad (2.88)$$

We then obtain the final boundary condition by applying Eq. (2.6) to Eq. (2.88), such that $\Phi_A(x) \sim e^{+i\omega x}$. This yields

$$B_+ e^{-3i\alpha_+} + B_- e^{-3i\alpha_-} = 0. \quad (2.89)$$

To solve for the aQNF, we treat Eqs. (2.87) and (2.89) as simultaneous equations. The aQNF expression emerges as

$$\left(i e^{\frac{3\pi i j}{2} + 2i\beta} + 3i e^{2i(\beta + \pi j)} + i e^{\frac{i}{2}(4\beta + \pi j)} + 3i e^{2i\beta} - 3e^{\frac{3\pi i j}{2} + 2i\omega x_0} + e^{2i(\omega x_0 + \pi j)} - 3e^{\frac{i}{2}(4\omega x_0 + \pi j)} + e^{2i\omega x_0} \right) \times e^{-i(\beta + \omega x_0 + \pi j)} = 0. \quad (2.90)$$

This is in agreement with Refs. [16, 26, 37, 38], where the solution for scalar- and tensor-modes of the gravitational aQNFs ($j = 0$) were found to be

$$\lim_{n \rightarrow \infty} \omega x_0 = \frac{\pi}{4} + \beta_+ - \arctan\left(\frac{i}{3}\right) + n\pi, \quad (2.91)$$

while the vector-modes ($j = 2$) yielded

$$\lim_{n \rightarrow \infty} \omega x_0 = \frac{3\pi}{4} + \beta_+ - \arctan\left(\frac{i}{3}\right) + n\pi \quad (2.92)$$

for $n \in \mathbb{N}$. These can be further generalised into a single expression,

$$\lim_{n \rightarrow \infty} \omega x_0 = \frac{\pi}{4}(d+1) - \arctan\left(\frac{i}{3}\right) + n\pi \quad (2.93)$$

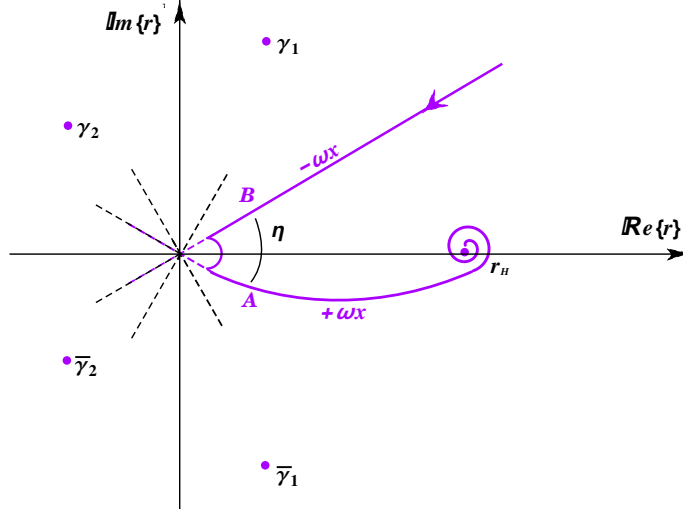


FIG. 7: *Anti-Stokes lines for a Schwarzschild AdS BH with $d = 6$.
Note the absence of a closed contour.*

for $n \in \mathbb{N}$, where the phase change of β_+ between solutions can be absorbed into $\pi(d+1)/4$ [16, 38].

While the aQNF of Eq. (2.90) holds true under the aforementioned circumstances, there are two known exceptions reported in Ref. [16], *viz.* the scalar-mode gravitational perturbations of the $d = 4$ and $d = 5$ Schwarzschild AdS BHs. For the former, the aQNF calculation yields

$$\lim_{n \rightarrow \infty} \omega x_0 = \frac{3\pi}{4} - \arctan\left(\frac{i}{3}\right) + n\pi \quad (n \in \mathbb{N}), \quad (2.94)$$

as j^∞ must be set to $+1$ rather than -1 [16]. For $d = 5$, we are required to select $j^\infty \rightarrow 0^+$. Consequently, $(1 \pm j^\infty)/2 > 0$, and the solution at $r \sim \infty$ therefore vanishes. This leaves but a single constraint, emerging from the BH horizon, which is insufficient to quantise the aQNFs. Thus, a continuous spectrum of aQNFs are produced (where $\omega \in \mathbb{C}$) for the 5D Schwarzschild AdS BH in the wake of spin-2 scalar-mode perturbations. In Ref. [26], these arguments were shown to apply also to the scalar-mode perturbations of electromagnetic fields.

III. BEHAVIOUR OF POTENTIALS NEAR SINGULAR POINTS

To reduce the effective BH QNM potentials developed in the literature to a generalised form, we extract only the dominant- r term of each potential and incorporate the appropriate

tortoise coordinate expression. In so doing, only the definition of the j (and j^∞) parameter(s) relays information about the spin of the perturbing field. We find that within the neighbourhood of the origin, the value of λ does not influence the outcome of the potential: all potentials take on the form given in Eq. (2.13). Near spatial infinity, however, the potentials in asymptotically flat BH spacetimes vanish; integer-spin and spin-3/2 perturbations in BH spacetimes with $\lambda \neq 0$ adopt a common form provided in Eq. (2.18).

A. Potentials of integer spin

In Refs. [43–46], Ishibashi and Kodama provide the effective potentials associated with the tensor-, vector-, and scalar-modes of the gravitational perturbations of d -dimensional, stationary, spherically-symmetric vacuum BH spacetimes. The vector- and scalar-modes are the higher-dimensional extensions of the axial/odd-parity and polar/even-parity modes, respectively, as described in Refs. [47–51, 64]. The tensor-mode of these spin-2 perturbations arises to account for the extra degrees of freedom beyond $d = 4$ and has been observed to possess the same form as the spin-0 (scalar) perturbations [3, 4]. Electromagnetic perturbations similarly require an additional scalar-mode potential, beyond the vector-mode that suffices for their 4D description, in higher dimensions; these are provided in Refs. [27, 65].

1. In the neighbourhood of $r \sim 0$

For the gravitational perturbations of Schwarzschild BHs inclusive and exclusive of a cosmological constant, we observe that the scalar- and tensor-modes collapse identically. The emergent form also describes the spin-0 perturbations. Thus,

$$V^s \sim V_T^{grav} \sim V_s^{grav} \sim \frac{f(r)}{r^2} \left[+ \frac{(d-2)^2 \mu}{2r^{d-3}} \right] \sim - \frac{(d-2)^2 \mu^2}{r^{2(d-2)}} \sim - \frac{1}{4x^2}, \quad (3.1)$$

$$V_V^{grav} \sim \frac{f(r)}{r^2} \left[- \frac{3(d-2)^2 \mu}{2r^{d-3}} \right] \sim + \frac{3(d-2)^2 \mu^2}{r^{2(d-2)}} \sim + \frac{3}{4x^2}, \quad (3.2)$$

such that $j_1 = 0$ and $j_2 = 2$, respectively [43, 44, 46].

From the electromagnetic perturbations of Schwarzschild BHs studied in Refs. [27, 65], we obtain

$$V_s^{EM} \sim \frac{f(r)}{r^2} \left[\frac{(d-2)(d-4)f(r)}{4} - \frac{(d-4)r}{2} f'(r) \right] \sim \frac{(3d-8)(d-4)}{4(d-2)^2 x^2}, \quad (3.3)$$

$$V_V^{EM} \sim \frac{f(r)}{r^2} \left[\frac{(d-4)(d-6)f(r)}{4} + \frac{(d-4)r}{2} f'(r) \right] \sim -\frac{d(d-4)}{4(d-2)^2 x^2}, \quad (3.4)$$

where $j_s = 2(d-3)/(d-2)$ and $j_v = 2/(d-2)$. As observed in Ref. [26], $j_s + j_v = 2$. Furthermore, as $d \rightarrow \infty$, $j_s \rightarrow 2$ and $j_v \rightarrow 0$: these are the j_i values corresponding to the scalar- and vector-modes of the gravitational perturbations, indicating that the scalar- and vector-modes of electromagnetic and gravitational fields become increasingly identical for higher dimensional contexts. Note also that $j_s = j_v = 1$ for $d = 4$, in keeping with the results of Ref. [25].

For the gravitational perturbations of Reissner-Nordström BHs inclusive and exclusive of a cosmological constant, spin-0, scalar- and tensor-modes of spin-2 perturbations share a common form; the vector-modes are expressed separately. Thus,

$$V^s \sim V_T^{grav} \sim V_{\pm s}^{grav} \sim -\frac{(d-2)(3d-8)}{4r^{4d-10}} \vartheta^4 \sim -\frac{(d-2)(3d-8)}{4(2d-5)^2 x^2}, \quad (3.5)$$

$$V_{\pm v}^{grav} \sim +\frac{(d-2)(5d-12)}{4r^{4d-10}} \vartheta^4 \sim +\frac{(d-2)(5d-12)}{4(2d-5)^2 x^2}, \quad (3.6)$$

for $j_1 = (d-3)/(2d-5)$ and $j_2 = (3d-7)/(2d-5)$. When $d = 4$, $V^s \sim -2\vartheta^4/r^6$ and $V_{\pm v}^{grav} \sim 4\vartheta^4/r^6$, in agreement with Ref. [25].

2. In the neighbourhood of $r \sim \infty$

From the potentials cited above, a universal term of $f(r)/r^2$ prefixes each expression. Since $f(r) \sim 1$ for both Schwarzschild and Reissner-Nordström BHs in asymptotically-flat space under the $r \sim +\infty$ condition, $V[r(x)] \sim 0$ near spatial infinity.

For Schwarzschild (A)dS BH spacetimes, we exploit $f(r) \sim -\lambda r^2$ and the subsequent expression for x given in Eq. (2.17) to claim that $\pm|\lambda|r \sim (x-x_0)^{-1}$, such that the potentials for the tensor-, vector-, and scalar-modes of the gravitational perturbations become

$$V^s \sim V_T^{grav} \sim \frac{f(r)}{r^2} \left[-\frac{d(d-2)}{4} \lambda r^2 \right] \sim \frac{-\lambda r^2}{r^2} \left[-\frac{d(d-2)}{4} \lambda r^2 \right] \sim \frac{(d-1)^2 - 1}{4(x-x_0)^2}, \quad (3.7)$$

$$V_s^{grav} = \frac{f(r)}{16r^2} \frac{U(r)}{H(r)^2} \sim -\frac{\lambda r^2}{16r^2} [-4\lambda r^2(d-4)(d-6)] \sim \frac{(d-5)^2 - 1}{4(x-x_0)^2}, \quad (3.8)$$

$$V_v^{grav} \sim \frac{f(r)}{r^2} \left[-\frac{(d-2)(d-4)}{4} \lambda r^2 \right] \sim \frac{(d-3)^2 - 1}{4(x-x_0)^2}. \quad (3.9)$$

Note that although the spin-0 and the tensor-mode of the spin-2 perturbations remain identical, we lose the commonality between gravitational scalar- and tensor-modes.

For the electromagnetic perturbations in Schwarzschild (A)dS BH spacetimes, we return to the expressions given in Ref. [65]. However, the dominant- r terms are now those containing the cosmological constant, such that

$$V_s^{EM} \sim \frac{f(r)}{r^2} \left[\frac{(d-2)(d-4)f(r)}{4} - \frac{(d-4)r}{2} f'(r) \right] \sim \frac{(d-5)^2 - 1}{4(x-x_0)^2}, \quad (3.10)$$

$$V_v^{EM} \sim \frac{f(r)}{r^2} \left[\frac{(d-4)(d-6)f(r)}{4} + \frac{(d-4)r}{2} f'(r) \right] \sim \frac{(d-3)^2 - 1}{4(x-x_0)^2}. \quad (3.11)$$

Here, we see that the scalar- and vector-modes of gravitational and electromagnetic perturbations have the same behaviour within the neighbourhood of spatial infinity, *viz.* $j_s^\infty = d-5$ and $j_v^\infty = d-3$, respectively. For scalar- and vector-modes of the electromagnetic perturbations, $(j_i^\infty)^2 = 1$ for $d=4$ such that the perturbation vanishes for $r \sim \infty$.

B. Potentials of half-integer spin

As observed in Ref. [66], the effective potentials corresponding to perturbing fields of half-integer spin can be expressed through

$$V_\pm = \pm F(r) \frac{d}{dr} W + W^2, \quad (3.12)$$

where W represents the superpotential and $F(r)$ is a function of $f(r)$. This expression applies to the Dirac fields, as well as to the Rarita-Schwinger fields studied in the gauge-invariant formalism of Refs. [67–70]. To compute the aQNFs via the monodromy technique, we approximate these QNM effective potentials into the form of Eqs. (2.13) and (2.18), and thereby extract the characteristic j behaviour. This can be achieved through a simple asymptotic analysis applied to spin-1/2 and spin-3/2 fields, where we consider both the transverse-traceless (TT) and non transverse-traceless (nonTT) eigenmodes of the latter.

1. In the neighbourhood of $r \sim 0$

From our study of integer perturbations within Schwarzschild BH spacetimes, we expect the potentials to approximate to $V[r(x)] \propto r^{-2(d-2)} \sim x^{-2}$. For spin-1/2 perturbations [71],

the superpotential yields expressions of the order of

$$W \propto \frac{r^{-(d-3)/2}}{r} = \frac{1}{r^{(d-1)/2}} \quad \Rightarrow \quad f(r) \frac{dW}{dr} \propto \frac{1}{r^{d-3}} \frac{1}{r^{(d+1)/2}} = \frac{1}{r^{(3d-5)/2}}, \quad (3.13)$$

such that

$$V_{\pm}^D \sim \pm f(r) \frac{dW}{dr} \propto \frac{1}{x^{(3d-5)/(2(d-2))}}, \quad (3.14)$$

with the incorporation of $r \propto x^{-(d-2)}$ from Eq. (2.14). By virtue of the fact that

$$\frac{3d-5}{2(d-2)} = \frac{3}{2} + \frac{1}{2(d-2)} < 2 \quad \forall d \geq 4, \quad (3.15)$$

we surmise that $j^2 - 1$ of Eq. (2.13) must vanish, such that $j = \pm 1$.

For spin-3/2 perturbations in Schwarzschild BH spacetimes, the superpotential of the TT eigenmodes is given by $W = \zeta \sqrt{f(r)}/r^2$, where ζ is the spinor-vector eigenvalue [68]. The Dirac analysis therefore applies to these potentials, such that $j = \pm 1$.

The superpotential of the nonTT eigenmodes [68], however, is

$$W = \frac{\sqrt{f(r)}}{r} \kappa \left[\frac{\kappa^2 - \frac{(d-2)^2}{4} \left(1 + \frac{d-4}{d-2} \frac{2\mu}{r^{d-3}}\right)}{\kappa^2 - \frac{(d-2)^2}{4} \left(1 - \frac{2\mu}{r^{d-3}}\right)} \right] \propto \frac{1}{r^{(d-1)/2}} [r^0], \quad (3.16)$$

where κ is related to the spinor eigenvalue on S^{d-2} (see Refs. [68] for details). The r -dependence of the superpotential is identical to that of the Dirac case. Consequently, $j = \pm 1$. Though the expressions for both the TT and nonTT eigenmodes of the spin-3/2 fields in Schwarzschild (A)dS BH spacetimes appear more complicated (see Refs. [53, 70]), they reduce in a similar fashion such that $j = \pm 1$ holds true.

From our study of integer fields in Reissner-Nordström BH spacetimes, we find that $V[r(x)] \propto r^{-2(2d-5)} \sim x^{-2}$. For the spin-1/2 perturbations [72], the superpotential yields expressions of the order of

$$W \propto \frac{r^{-(d-3)}}{r} = \frac{1}{r^{d-2}} \quad \Rightarrow \quad f(r) \frac{dW}{dr} \propto \frac{1}{r^{2(d-3)}} \frac{1}{r^{d-1}} = \frac{1}{r^{3d-7}}, \quad (3.17)$$

such that

$$V_{\pm}^D \sim \pm f(r) \frac{dW}{dr} \propto \frac{1}{x^{(3d-7)/(2d-5)}}, \quad (3.18)$$

with the incorporation of $r \propto x^{-(2d-5)}$ from Eq. (2.15). By virtue of the fact that

$$\frac{3d-7}{2d-5} = \frac{3}{2} + \frac{1}{2(2d-5)} < 2 \quad \forall d \geq 4, \quad (3.19)$$

we surmise that $j^2 - 1$ of Eq. (2.13) must vanish, such that $j = \pm 1$.

For spin-3/2 perturbations in Reissner-Nordström BH spacetimes, as studied in Ref. [69], the superpotential associated with the nonTT eigenmodes becomes

$$W = \frac{\sqrt{f(r)}}{r} \left(\kappa + \frac{d-2}{2} \frac{\vartheta}{r^{d-3}} \right) \left[1 + \frac{(d-2)(d-3)}{2 \left(\kappa + \frac{d-2}{2} \frac{\vartheta}{r^{d-3}} \right)} \left(\frac{(1-f(r))\kappa + \frac{d-2}{2} \frac{\vartheta}{r^{d-3}}}{\frac{(d-2)^2}{4} f(r) - \left(\kappa + \frac{d-2}{2} \frac{\vartheta}{r^{d-3}} \right)^2} \right) \right] \\ \sim \frac{\vartheta^2}{r^{2d-5}} \left(\frac{d-2}{2} \right) \left(\frac{(d-2)^2 \mu + 2(2d-5)\vartheta\kappa}{(d-2)^2 \mu + 2(d-2)\vartheta\kappa} \right) \quad (3.20)$$

when $r \sim 0$. Here, both $f(r)dW/dr$ and W^2 contribute equally to the nonTT spin-3/2 potential. With the incorporation of $\vartheta^4/r^{4d-10} \sim (2d-5)^2 x^2$ (see eq. (2.15)),

$$V_+^{RS_{non}} \sim - \frac{[(d-2)^2 \mu + 2(2d-5)\vartheta\kappa] [(3d-8)(d-2)\mu + 2(2d-5)\vartheta\kappa]}{4((d-2)^2 \mu + 2\vartheta\kappa)^2 (2d-5)^2 x^2}, \quad (3.21)$$

$$V_-^{RS_{non}} \sim + \frac{[(d-2)^2 \mu + 2(2d-5)\vartheta\kappa] [(5d-12)(d-2)\mu + 6(2d-5)\vartheta\kappa]}{4((d-2)^2 \mu + 2\vartheta\kappa)^2 (2d-5)^2 x^2}. \quad (3.22)$$

Throughout this work, the superscript RS_{non} denotes non-TT Rarita Schwinger perturbations. Despite the complicated nature of the expressions, these potentials may still be reduced to the form of eq. (2.13), where

$$j_+ = \frac{(d-3)(d-2)\mu}{((d-2)\mu + 2\vartheta\kappa)(2d-5)}, \quad (3.23)$$

$$j_- = \frac{(3d-7)(d-2)\mu + 4(2d-5)\vartheta\kappa}{((d-2)\mu + 2\vartheta\kappa)(2d-5)}, \quad (3.24)$$

for $V_+^{RS_{non}}$ and $V_-^{RS_{non}}$, respectively.

We note with interest that in the $\mu \gg \vartheta\kappa$ limit,

$$V_+^{RS_{non}} \Big|_{\mu \gg \vartheta\kappa} \equiv \tilde{V}_+^{RS_{non}} \sim - \frac{(3d-8)(d-2)}{4(2d-5)^2 x^2}, \quad (3.25)$$

$$V_-^{RS_{non}} \Big|_{\mu \gg \vartheta\kappa} \equiv \tilde{V}_-^{RS_{non}} \sim + \frac{(5d-12)(d-2)}{4(2d-5)^2 x^2}. \quad (3.26)$$

We shall use a tilde to denote expressions in this limit. These potentials are identical to the scalar-/tensor- and vector-modes of the gravitational perturbations of the Reissner-Nordström BH spacetime, respectively. As such, we find that $\tilde{j}_+ = (d-3)/(2d-5)$ and $\tilde{j}_- = (3d-7)/(2d-5)$. Furthermore, we find that $\tilde{V}_+^{RS_{non}} = -2\vartheta^4/r^6$ for $d=4$ in this limit, which is equivalent to the 4D spin-3/2 result of Ref. [25].

For the TT spin-3/2 eigenmodes in Reissner-Nordström BH spacetimes,

$$W = \frac{\sqrt{f(r)}}{r} \left(\zeta - \frac{d-2}{2} \frac{\vartheta}{r^{d-3}} \right) \sim - \frac{d-2}{2} \frac{\vartheta^2}{r^{2d-5}}. \quad (3.27)$$

Thus,

$$V_+^{RS_{TT}} \sim + \left(\frac{\vartheta^2}{r^{2d-6}} \right) \frac{d}{dr} \left(-\frac{d-2}{2} \frac{\vartheta^2}{r^{2d-5}} \right) + \frac{(d-2)^2}{4} \frac{\vartheta^4}{r^{4d-10}} \sim + \frac{(d-2)(5d-12)}{4(2d-5)^2 x^2} \quad (3.28)$$

$$V_-^{RS_{TT}} \sim - \left(\frac{\vartheta^2}{r^{2d-6}} \right) \frac{d}{dr} \left(-\frac{d-2}{2} \frac{\vartheta^2}{r^{2d-5}} \right) + \frac{(d-2)^2}{4} \frac{\vartheta^4}{r^{4d-10}} \sim - \frac{(d-2)(3d-8)}{4(2d-5)^2 x^2} . \quad (3.29)$$

Here, $j_+ = (3d-7)/(2d-5)$ for $V_+^{RS_{TT}}$ and $j_- = (d-3)/(2d-5)$ for $V_-^{RS_{TT}}$, which also correspond to the vector- and scalar-/tensor modes of the gravitational perturbations, respectively. As such, $V_{\pm}^{RS_{TT}}$ matches $\tilde{V}_{\mp}^{RS_{non}}$ within the neighbourhood of the origin.

2. In the neighbourhood of $r \sim \infty$

As in the case of integer-spin fields, $f(r) \sim 1$ for both Schwarzschild and Reissner-Nordström BHs in asymptotically-flat space under the $r \sim +\infty$ condition. As such, $V[r(x)] \sim 0$ near spatial infinity.

In (A)dS BH spacetimes, $f(r) \sim -\lambda r^2$ near spatial infinity. Thus, for spin-1/2 perturbations in Schwarzschild and Reissner-Nordström BHs inclusive of a cosmological constant,

$$\begin{aligned} W &\sim \frac{\sqrt{-\lambda r^2}}{r} \kappa = (-\lambda)^{1/2} \kappa \\ &\Rightarrow V_{\pm}^D \sim \lambda \kappa^2 . \end{aligned} \quad (3.30)$$

With $V_{\pm}^D \propto r^0$ for both Schwarzschild (A)dS and Reissner-Nordström (A)dS BH spacetimes, we consider $j^{\infty} = \pm 1$.

For spin-3/2 perturbations in Schwarzschild (A)dS BH spacetimes [70], we consider

$$V_{\mp}^{RS_{non}} = \mp \partial_x W + W^2 , \quad W = [\mathcal{D}^2 - \mathcal{B}^2]^{1/2} f^{-1} \mathcal{F} , \quad (3.31)$$

for the nonTT eigenmodes. Here, $\partial_x = \mathcal{F} \partial_r$, for which

$$\mathcal{F} = f(r) \left[1 + \frac{f(r)}{2\omega} \left(\frac{\partial}{\partial r} \frac{\mathcal{D}}{i\mathcal{B}} \right) \left(\frac{\mathcal{B}^2}{\mathcal{B}^2 - \mathcal{D}^2} \right) \right]^{-1} . \quad (3.32)$$

Since the asymptotic limit demands that $|\omega| \rightarrow +\infty$, we may approximate $\mathcal{F} \approx f(r)$. Thus, $W = [\mathcal{D}^2 - \mathcal{B}^2]^{1/2}$.

With the use of

$$z = \frac{-\frac{(d-3)(d-2)}{2} \frac{2\mu}{r^{d-3}}}{\kappa^2 - \frac{(d-2)^2}{4} \left(1 - \frac{2\mu}{r^{d-3}} \right)} \propto 0 , \quad (3.33)$$

we may reduce \mathcal{D} and \mathcal{B} in the following manner:

$$\mathcal{B} = i\kappa \frac{\sqrt{f(r)}}{r} (z+1) \sim i(-\lambda)^{1/2} \kappa, \quad (3.34)$$

$$\mathcal{D} = -i\sqrt{\lambda f(r)} \frac{(d-2)}{2} \left(z + \frac{d-4}{d-2} \right) \sim -i \frac{(d-4)}{2} (-\lambda^2)^{1/2} r = \frac{(d-4)}{2} |\lambda| r. \quad (3.35)$$

Therefore,

$$W \sim \sqrt{\frac{(d-4)^2}{4} \lambda^2 r^2 - \lambda \kappa^2} \sim \frac{(d-4)}{2} |\lambda| r, \quad (3.36)$$

such that

$$V_-^{RS_{non}} = -\partial_x W + W^2 \sim -(-\lambda r^2) \frac{(d-4)}{2} |\lambda| + \frac{(d-4)^2}{4} |\lambda|^2 r^2 \sim \frac{(d-4)(d-6)}{4(x-x_0)^2}, \quad (3.37)$$

$$V_+^{RS_{non}} = +\partial_x W + W^2 \sim +(-\lambda r^2) \frac{(d-4)}{2} |\lambda| + \frac{(d-4)^2}{4} |\lambda|^2 r^2 \sim \frac{(d-2)(d-4)}{4(x-x_0)^2}. \quad (3.38)$$

Note that we have imposed $-\lambda = |\lambda|$ within the potentials, in keeping with the arguments of Ref. [53]. From $V_-^{RS_{non}}$ and $V_+^{RS_{non}}$, respectively, we determine that $j_-^\infty = d-5$ and $j_+^\infty = d-3$. The behaviour of $V_-^{RS_{non}}$ corresponds to V_s^{grav} and V_s^{EM} while $V_+^{RS_{non}}$ matches that of V_v^{grav} and V_v^{EM} near spatial infinity.

Similarly, for the TT eigenmodes,

$$V_{\mp}^{RS_{TT}} = \mp \partial_x \mathbb{W} + \mathbb{W}^2, \quad \mathbb{W} = [\mathbb{D}^2 - \mathbb{B}^2]^{1/2} f^{-1} \mathbb{F}, \quad (3.39)$$

where $\partial_x = \mathbb{F} \partial_r$, with

$$\mathbb{F} = f(r) \left[1 + \frac{f(r)}{2\omega} \left(\frac{\partial}{\partial r} \frac{\mathbb{D}}{i\mathbb{B}} \right) \left(\frac{\mathbb{B}^2}{\mathbb{B}^2 - \mathbb{D}^2} \right) \right]^{-1}. \quad (3.40)$$

We once again claim that $|\omega| \rightarrow +\infty$ implies $\mathbb{F} \sim f(r)$. Thus, $W \sim [\mathbb{D}^2 - \mathbb{B}^2]^{1/2}$.

We may reduce \mathbb{D} and \mathbb{B} in the following manner:

$$\mathbb{B} = i\zeta \frac{\sqrt{f(r)}}{r} \sim i(-\lambda)^{1/2} \zeta, \quad (3.41)$$

$$\mathbb{D} = -i\sqrt{\lambda f(r)} \frac{(d-2)}{2} \sim -i \frac{(d-2)}{2} (-\lambda^2)^{1/2} r = \frac{(d-2)}{2} |\lambda| r \quad (3.42)$$

Then

$$\mathbb{W} \sim \sqrt{\frac{(d-2)^2}{4} \lambda^2 r^2 - \lambda \zeta^2} \sim \frac{(d-2)}{2} |\lambda| r, \quad (3.43)$$

such that

$$V_-^{RS_{TT}} = -\partial_x \mathbb{W} + \mathbb{W}^2 \sim -(-\lambda r^2) \frac{(d-2)}{2} |\lambda| + \frac{(d-2)^2}{4} |\lambda|^2 r^2 \sim \frac{(d-2)(d-4)}{4(x-x_0)^2}, \quad (3.44)$$

$$V_+^{RS_{TT}} = +\partial_x \mathbb{W} + \mathbb{W}^2 \sim +(-\lambda r^2) \frac{(d-2)}{2} |\lambda| + \frac{(d-2)^2}{4} |\lambda|^2 r^2 \sim \frac{d(d-2)}{4(x-x_0)^2}. \quad (3.45)$$

Note that we have once again imposed $-\lambda = |\lambda|$ within the potentials, in keeping with the arguments of Ref. [53]. From $V_-^{RS_{TT}}$ and $V_+^{RS_{TT}}$, respectively, we determine that $j_-^\infty = d - 3$ and $j_+^\infty = d - 1$. The behaviour of $V_+^{RS_{TT}}$ matches that of V^s and V_T^{grav} while $V_-^{RS_{TT}}$ corresponds to V_V^{grav} , V_V^{EM} , and $V_+^{RS_{non}}$ near spatial infinity.

IV. AQNF EXPRESSIONS OF SPHERICALLY-SYMMETRIC BH SPACETIMES

The final results for QNFs corresponding to perturbing fields of spin $s \in \{0, 1/2, 1, 3/2, 2\}$ within the large- n limit are produced by incorporating the appropriate expressions of j (and j^∞) into the generalised aQNF expressions of subsection II C. Where j is a dimensionally-independent parameter, the aQNF expressions may be considered applicable for $d > 3$ [16]. However, since most aQNF expressions feature dimensionally-dependent j and j^∞ parameters, we specify that such results hold provided their associated perturbing fields are stable within the BH spacetime of interest (see Table I of Ref. [46] and Table IV of Ref. [4] for known stable contexts). As far as possible, we validate our new half-integer results against extant aQNF expressions available in the literature.

Note that in the following tables (Tables II-VI), horizontal lines demarcate common final aQNF solutions: when the specified j and/or j^∞ value(s) are substituted into the equation provided for some specified d , the aQNF output is identical for grouped perturbations.

A. aQNFs of the Schwarzschild BH spacetimes

To calculate the highly-damped QNFs of the Schwarzschild BH spacetime, we use Eq. (2.54). For the spin-0, spin-2, spin-1/2, and spin-3/2 perturbations, the j values are dimensionally-independent; if Eq. (2.54) holds, then these solutions of Table II remain consistent for all $d > 3$.

While the scalar- and vector-modes of the spin-1 perturbations consistently yield aQNF expressions equivalent to one another, these results vary from dimension to dimension. For $d = 6$, we observe that the real part vanishes and only a $2\pi iT_H(n + 1/2)$ term remains. When $d = 5$, an ill-defined $\ln(0)$ emerges. This was observed in Ref. [26], where López-Ortega suggested that the $\ln(0)$ term was a consequence of the real part of the QNF rapidly

TABLE II: For the highly-damped QNFs within the Schwarzschild BH spacetime, only the electromagnetic perturbations exhibit dimensional dependence. Irrespective of the perturbing mode or chirality of the QNM potential, the aQNFs of each spin reduce to a common form.

<i>potential</i>	$\pm j$	$\lim_{n \rightarrow \infty} \omega \quad (n \in \mathbb{N})$
$V^s, V_T^{grav}, V_S^{grav}$	0	$T_H \ln 3 + 2\pi i T_H (n + \frac{1}{2})$
V_V^{grav}	2	
V_S^{EM}	$\frac{2(d-3)}{d-2}$	$T_H \ln(-1 - 2 \cos(\pi j)) + 2\pi i T_H n$
V_V^{EM}	$\frac{2}{d-2}$	
$V_{\pm}^D, V_{\pm}^{RSnon}, V_{\pm}^{RSTT}$	1	$2\pi i T_H n$

reducing to zero, citing the numerical work of Ref. [9]. For the 4D case, the electromagnetic j reduces to 1 and the aQNF becomes $2\pi i T_H n$, in agreement with Ref. [25]. Once $d > 6$, the argument of the natural logarithm remains greater than 1 such that the real part of the aQNF cannot be dismissed.

Moreover, we note that Eq. (1.1) holds for the Schwarzschild BH, irrespective of the spin of the perturbing field. The offset for the scalar and gravitational aQNFs remains $\ln 3$ while the gap is given by $2\pi i T_H = ik_H$. The newly-computed half-integer results (and the spin-1 aQNFs in the $d = 4, 6$ contexts), however, have an offset of zero. These are in agreement with the 4D results of Ref. [25]. The oscillation frequency of the emitted radiation therefore cannot be extracted from these highly-damped QNFs, as they are purely imaginary.

B. aQNFs of the Reissner-Nordström and extremal Reissner-Nordström BHs

For the non-extremal Reissner-Nordström BH spacetimes, we compute the aQNFs of spin $s \in \{0, 1/2, 3/2, 2\}$ via Eq. (2.77). In Table III we then demonstrate that our Rarita-Schwinger results match those of the gravitational aQNFs. This can be inferred from section III, where the \tilde{j} parameters extracted from the spin-3/2 nonTT-modes subjected to the

TABLE III: For the highly-damped QNFs within the non-extremal Reissner-Nordström BH spacetime, only the spin-1/2 aQNFs are dimensionally-independent. The aQNFs of spin $s \in \{0, 3/2, 2\}$ reduce to a common form for all but the unmodified nonTT spin-3/2 modes, irrespective of the perturbing mode or chirality. Demarcated rows represent common results.

<i>potential</i>	$\pm j$	$e^{+\frac{2\pi\omega}{k_H^+}}$
$V^s, V_{\pm S}^{grav}, V_T^{grav}, \tilde{V}_+^{RS_{non}}, V_-^{RS_{TT}}$	$\frac{d-3}{2d-5}$	Eq. (2.77)
$V_{\pm V}^{grav}, \tilde{V}_-^{RS_{non}}, V_+^{RS_{TT}}$	$\frac{3d-7}{2d-5}$	
$V_+^{RS_{non}}$	$\frac{(d-3)(d-2)\mu}{((d-2)\mu + 2\vartheta\kappa)(2d-5)}$	Eq. (2.77)
$V_-^{RS_{non}}$	$\frac{(3d-7)(d-2)\mu + 4(2d-5)\vartheta\kappa}{((d-2)\mu + 2\vartheta\kappa)(2d-5)}$	Eq. (2.77)
V_{\pm}^D	1	1

$\mu \gg \vartheta\kappa$ limit ($\tilde{V}_{\pm}^{RS_{non}}$) were shown to be equivalent to the j parameters of the TT-modes with opposing chirality ($V_{\mp}^{RS_{TT}}$). As such, $\tilde{V}_+^{RS_{non}}$ ($V_-^{RS_{TT}}$) corresponds to spin-0 and the scalar- and tensor-modes of the spin-2 perturbations while $\tilde{V}_-^{RS_{non}}$ ($V_+^{RS_{TT}}$) corresponds to the spin-2 vector-modes. The aQNFs follow suit.

Irrespective of the mode of the perturbing field, the aQNFs of spin $s \in \{0, 3/2, 2\}$ reduce to a common aQNF expression for all $d > 3$, which differs from dimension to dimension. For $d \geq 5$, the aQNFs of spin $s \in \{0, 3/2, 2\}$ cannot be solved analytically. For the nonTT modes of the spin-3/2 aQNFs, these observations apply only if $\mu \gg \vartheta\kappa$.

When $d = 4$, the aQNFs of spin $s \in \{0, 3/2, 2\}$ within the Reissner-Nordström BH spacetime reduce to

$$e^{\frac{2\pi\omega}{k_H^+}} = -2 - 3e^{-\frac{2\pi\omega}{k_H^-}}, \quad (4.1)$$

which corresponds to the results of Ref. [25]. Note that for this 4D result, the spin-3/2 aQNF is calculated from \tilde{V}_+^{non} .

For the spin-1/2 aQNFs,

$$e^{\pi\omega/k_H^+} = 1 \quad \Rightarrow \quad \lim_{n \rightarrow +\infty} \omega = 2\pi i T_H n \quad (4.2)$$

holds, irrespective of d . This is in agreement with the 4D results of Ref. [25], since only k_H^+ contributes to T_H . As in the Schwarzschild case, we find Dirac aQNFs that are purely imaginary, with a gap given by a multiple of the Hawking temperature. Note that this result therefore ignores the surface gravity of the Cauchy horizon, such that the spin-1/2 aQNFs allow for an isolated study of the surface gravity of the outer horizon.

However, we note that if the $\mu \gg \vartheta\kappa$ limit is not imposed, the nonTT spin-3/2 results in non-extremal Reissner-Nordström BHs showcase discrepancies from the other aQNFs demonstrated here. Though they differ from dimension to dimension, these spin-3/2 aQNFs of opposing chiralities do not match one another. Furthermore, these retain their dependence on the BH mass and charge, as well as on the spinor eigenvalue on S^{d-2} . Such features in the aQNF are to be expected from the form of the \tilde{j} parameters of Eqs. (3.23) and (3.24), which are distinct from one another and dependent on ϑ , μ , and κ .

In the case of the extremal Reissner-Nordström BH spacetimes, the aQNFs can be computed using Eq. (2.82). These results are compiled in Table IV, where identical aQNF outputs are indicated by shared rows. The aQNFs of spin $s \in \{0, 3/2, 2\}$ manifest in the form of

$$\lim_{n \rightarrow \infty} \omega = T \ln[\text{trigonometric function}] + 2\pi i T[\text{gap}] .$$

Spin-0,2 and TT spin-3/2 aQNFs have a common real part. Specifically,

$$\ln(2) < \mathbb{R}e\left\{ \lim_{n \rightarrow \infty} \left\{ \lim_{n \rightarrow \infty} \omega \right\} \right\} \leq \ln(3) ,$$

where the natural logarithm decreases from $\ln(3)$ for $d = 4$ with increasing d . For $\kappa = 0$, the nonTT spin-3/2 aQNFs are equivalent to their TT counterparts for each $d \geq 4$. For a fixed d but increasing κ , the magnitude of the real part of the nonTT spin-3/2 aQNF increases from $\ln(3.7321)$ for $\kappa = 1$ (and $d = 4$). As such, for $\kappa \neq 0$, the aQNFs of the nonTT spin-3/2 fields decrease (increase) with increasing d (κ) with other parameters fixed in the range

$$\ln(2) < \mathbb{R}e\left\{ \lim_{n \rightarrow \infty} \omega \right\} < \ln(4) .$$

$V_-^{RS_{non}}$ and $V_+^{RS_{non}}$ are isospectral.

TABLE IV: For the highly-damped QNFs within the extremal Reissner-Nordström BH spacetime, the aQNFs of spin $s \in \{0, 3/2, 2\}$ reduce to a common form. The spin-1/2 aQNFs are ill-defined. Demarcated rows represent shared results.

<i>potential</i>	$\pm j$	$e^{\frac{2\pi\omega}{k}}$
$V^s, V_{\pm S}^{grav}, V_T^{grav}, V_-^{RS_{TT}}$	$\frac{d-3}{2d-5}$	Eq. (2.82)
$V_{\pm V}^{grav}, V_+^{RS_{TT}}$	$\frac{3d-7}{2d-5}$	
$V_+^{RS_{non}}$	$\frac{(d-3)(d-2)}{(2d-5)(d-2+2\kappa)}$	Eq. (2.82)
$V_-^{RS_{non}}$	$\frac{(3d-7)(d-2)+4(2d-5)\kappa}{(2d-5)(d-2+2\kappa)}$	Eq. (2.82)
V_{\pm}^D	1	0

The gap for spin-0,2 and TT spin-3/2 aQNFs is given by $2\pi iT(n + 1/2)$; for nonTT spin-3/2 aQNFs, it is $2\pi iTn$ for all κ, d .

Thus, these spin $s \in \{0, 3/2, 2\}$ aQNFs of the extremal Reissner-Nordström BH spacetime resemble the Schwarzschild form more so than the aQNFs of any other spacetime, albeit with a trigonometric function as the argument of the natural logarithm rather than an integer. This applies for all $d \geq 4$ cases computed. For the special case of $d = 4$ for the spin-0,2 aQNFs, we find that the $\Re\{\omega\} \sim \ln 3$ result is recovered, in agreement with Refs. [13, 59]. However, as explained in subsection IIC2, an attempt to link these results to Hod's conjecture would be invalid since the underlying arguments thereof are based on Bekenstein and Mukhanov's BH area quantisation [32–34], which itself is predicated on non-extremal BH spacetimes. In subsection IIC2 we also discussed the $T = k/2\pi$ function that is analogous – but not equivalent – to the Hawking temperature.

For the spin-1/2 aQNFs, we once again observe dimensional independence. However, since Eq. (2.82) reduces to $e^{2\pi\omega/k} = 0$, the aQNF spectrum is ill-defined. The reasoning for this is unclear and demands further investigation.

As indicated by Cho in Ref. [25], the shared forms recorded in Table IV for aQNFs of spin $s \in \{0, 3/2, 2\}$ for the extremal Reissner-Nordström BH spacetimes may indicate a connection to SUSY frameworks.

On the basis of the inherent characteristics of the extremal Reissner-Nordström BH related to supergravity conjectures [63, 73–75], Onozawa *et al.* in Ref. [62] associated the isospectrality between photon, graviton, and gravitino QNFs observed in the 4D extremal Reissner-Nordström BHs [60] with a manifestation of a hidden $\mathcal{N} = 2$ SUSY. In particular, they considered that since the extremal Reissner-Nordström BH admits a Killing spinor field [75], the background solution is expected to be invariant under SUSY transformations with respect to this Killing spinor field. Consequently, all perturbed fields would be expected to be related via SUSY transformations that conserve the S-matrix. In the case of Refs. [60, 62], the SUSY transformation was an increase of $1/2$ in the multipolar index, corresponding to an increase of $1/2$ in the spin of the field. Cho in Ref. [25] considered that this could relate to the commonality observed between QNFs of $s \in \{1, 3/2, 2\}$ within the large overtone limit, but could not find a clear way to demonstrate that between the scalar and Dirac aQNFs.

Although our results concern higher-dimensional QNFs within the large overtone limit, the shared form between spin-2 and spin-3/2 results observed in Table IV may indicate some manifestation of SUSY beyond the known $d = 4$ results (particularly in the wake of the extension of SUSY qualities to extremal Reissner-Nordström BHs in higher dimensions [76]). Whether this commonality also extends to the electromagnetic aQNFs in these BH spacetimes is an open question and motivates for the development of effective QNM potentials for electromagnetic perturbations within higher dimensional Reissner-Nordström BH spacetimes.

By virtue of the consistent j parameter in most cases, we observe that Tables III and IV showcase the same shared behaviour between potentials. However, since we expect only extreme BHs to preserve SUSY [62], the connection between supergravity considerations and uniform aQNFs applies only to the extremal Reissner-Nordström BH context.

TABLE V: For the highly-damped QNFs within the Schwarzschild dS BH spacetime, the spin-0 and spin-2 aQNFs are dimensionally-independent and reduce to an identical form. This is also the case for all half-integer aQNFs. A common aQNF expression emerges for the scalar- and vector-modes of the spin-1 aQNFs, varying from dimension to dimension.

<i>potential</i>	$\pm j$	<i>aQNF</i>
$V^s, V_T^{grav}, V_S^{grav}$	0	$\cosh\left(\frac{\pi\omega}{k_H} - \frac{\pi\omega}{k_C}\right) + 3 \cosh\left(\frac{\pi\omega}{k_H} + \frac{\pi\omega}{k_C}\right) = 0$
V_V^{grav}	2	
V_S^{EM}	$\frac{2(d-3)}{d-2}$	Eq. (2.62)
V_V^{EM}	$\frac{2}{d-2}$	
$V_{\pm}^D, V_{\pm}^{RS_{non}}, V_{\pm}^{RS_{TT}}$	1	$2\pi iT_H n$ or $-2\pi iT_C n$

C. aQNFs of the Schwarzschild dS and Schwarzschild AdS BH spacetimes

We may compute the aQNFs of the Schwarzschild dS BH using Eq. (2.61). Within Table V we observe that the spin-2 and spin-0 results are uniform for all d , as demonstrated in Refs. [16, 37]. This aQNF expression, however, cannot be solved analytically.

The scalar- and vector-modes of the spin-1 aQNFs yield a common result. For $d = 4, 5, 6$, the real part is zero and the gap is a function of the surface gravity of either the event or cosmological horizon. This is in agreement with Refs. [9, 26]. For example, the highly-damped QNFs of the electromagnetic scalar- and vector-modes become

$$\lim_{n \rightarrow \infty} \omega = 2\pi iT_H \left(n + \frac{1}{2}\right) \quad \text{or} \quad \lim_{n \rightarrow \infty} \omega = -2\pi iT_C \left(n + \frac{1}{2}\right) \quad (4.3)$$

when $d = 6$ and using $k_C = 2\pi T_C < 0$.

We note with interest that the newly-computed half-integer aQNFs share a common, dimensionally-independent expression in the Schwarzschild dS BH spacetime that closely resembles that of the spin-1 case for $d = 4, 5, 6$, *viz.*

$$\lim_{n \rightarrow \infty} \omega = 2\pi iT_H n \quad \text{or} \quad \lim_{n \rightarrow \infty} \omega = -2\pi iT_C n. \quad (4.4)$$

TABLE VI: *The aQNFs within the Schwarzschild AdS BH spacetime. While the structure of the expressions remains consistent, the argument of the arctan and the phase shift differs from dimension to dimension. Here, we provide results for $d = 6$ in the rightmost column.*

<i>potential</i>	$\pm j$	$\pm j^\infty$	$\lim_{n \rightarrow \infty} \omega x_0 \ (n \in \mathbb{N})$
V^s, V_T^{grav}	0	$(d-1)$	$\frac{7\pi}{4} - \arctan\left(\frac{i}{3}\right) + n\pi$
V_V^{grav}	2	$(d-3)$	
V_S^{grav}	0	$(d-5)$	$\frac{3\pi}{4} - \arctan\left(\frac{i}{3}\right) + n\pi$
V_S^{EM}	$\frac{2(d-3)}{d-2}$	$(d-5)$	$\frac{\pi}{2} + \arctan\left(\frac{3+4i}{5}\right) + n\pi$
V_V^{EM}	$\frac{2}{d-2}$	$(d-3)$	$\pi + \arctan\left(\frac{3+4i}{5}\right) + n\pi$
V_\pm^D	1	1	$\frac{\pi}{2} - \arctan\left(\frac{3+4i}{5}\right) + n\pi$
$V_-^{RS_{non}}$		$(d-5)$	$\frac{\pi}{2} - \arctan\left(\frac{3+4i}{5}\right) + n\pi$
$V_+^{RS_{non}}, V_-^{RS_{TT}}$		$(d-3)$	$\pi - \arctan\left(\frac{3+4i}{5}\right) + n\pi$
$V_+^{RS_{TT}}$		$(d-1)$	$\frac{3\pi}{2} - \arctan\left(\frac{3+4i}{5}\right) + n\pi$

In fact, when reduced to the 4D context, the spin-1 aQNFs reflect the spin-1/2 and spin-3/2 results exactly.

As discussed in subsection [II C 1](#), the 5D case does require its own analysis and yields a slightly different expression for the aQNF. Therein, we have also demonstrated that the Schwarzschild aQNF may be extracted from Eq. [\(2.61\)](#) if subjected to the $\lambda \rightarrow 0^+$ limit.

For the Schwarzschild AdS BH, the aQNFs can be produced using Eq. [\(2.90\)](#). There is a pronounced uniformity in the structure of these expressions: irrespective of the spin of the field, the aQNFs have a consistent form marked by an arctan and a phase shift. However, since the specific argument of the arctan and the phase shift differs from dimension to dimension, we have provided the explicit aQNF expressions for the $d = 6$ case in Table [VI](#).

The gravitational perturbations have been confirmed against the results of Refs. [16, 37, 38], where we note that the $i \ln(2)/2$ of Ref. [38] is equivalent to $\arctan(i/3)$, and the sign difference is due to their use of a negative temporal dependence. As such, for the gravitational and scalar aQNFs, only the phase shift contributes to the real part of $\omega x_0|_{n \rightarrow \infty}$. For fields of $s \in \{1/2, 1, 3/2\}$, however, we find that the argument of this arctan incorporates real and imaginary parts, which increases the magnitude of the real part of the aQNF. Note, however, that the sign of the arctan is positive only for aQNFs of the electromagnetic field.

Finally, we add that there are not many analytic studies available for the aQNFs of BH spacetimes inclusive of a cosmological constant (however, see section 3.2.1 of Ref. [16] for a thorough review of the numerical results for the Schwarzschild AdS QNF), which makes these results particularly useful. However, it must be noted that the Schwarzschild AdS aQNFs are derived using the Dirichlet boundary conditions. As discussed in Ref. [53], the influence of boundary conditions in AdS BH spacetimes can have a profound effect on the computational output. Whether the application of these boundary conditions yields the most physically appropriate aQNFs requires additional consideration.

V. CONCLUSIONS

Although highly-damped QNMs are not observable, the application of asymptotic limits allows for the isolation of real and imaginary behaviours. For our study of aQNFs, we opted to pursue the monodromy technique pioneered in Ref. [15], which can be considered as a more economical iteration of the “phase-integral” method of Andersson and Howls [13].

In our explicit review of the application of the method to Schwarzschild, Reissner-Nordström, and Schwarzschild (A)dS BHs, we observed that the BH family dictates the behaviour near the origin (see Table I) while the cosmological constant determines the behaviour near spatial infinity (see Eq. (2.17)). This is observable also from section III, where the exploitation of the appropriate tortoise coordinate allows for the approximation of QNM potentials from the literature into the form of Eq. (2.13) dependent on a field-specific parameter j . As such, the computation of aQNFs via the monodromy technique remains uniform for perturbations of spin s : the topology of the complex plane, the contour traced, and the boundary conditions applied depend solely on the BH metric function; the contribution from the field is included once the generalised aQNF expression has been computed, via the j

and j^∞ parameters.

With these principles in place, we computed the aQNFs of spin $s \in \{0, 1/2, 1, 3/2, 2\}$, where all half-integer aQNFs reflect new results. As in the integer-spin cases, the j and j^∞ parameters for the half-integer perturbations were extracted through an asymptotic analysis of the QNM effective potentials. For Schwarzschild, non-extremal Reissner-Nordström, and Schwarzschild dS BH spacetimes, we observed that the Dirac aQNFs emerged consistently as a purely imaginary solution proportional to the surface gravity of the horizon for all but the Schwarzschild AdS and extremal Reissner-Nordström BH spacetimes. This consistency in the Dirac aQNFs is particularly interesting as it defies the general trend observed in our results *viz.* that the final aQNF solution depends more on the BH spacetime than the spin of the perturbing field. Furthermore, we observe that the Rarita-Schwinger behaviour corresponds predominantly to that of the Dirac field (demonstrable in the cases of Schwarzschild and Schwarzschild (A)dS BHs), but matches precisely the gravitational perturbations for other BH spacetimes. Specifically, aQNFs associated with $V_-^{TT}(\tilde{V}_+^{non})$ and $V_+^{TT}(\tilde{V}_-^{non})$ corresponded to $V_{\pm S,T}^{grav}$ and $V_{\pm V}^{grav}$, respectively. The justification for these observed behaviours is not obvious and warrants further investigation.

Except for most Dirac aQNFs, and the spin-1 aQNFs of the Schwarzschild dS BH, we have found that the structure of the aQNF solutions is consistent for each spacetime, irrespective of the spin of the perturbing field. We observe in several cases that the real part tends to a finite value, while the imaginary part grows in fixed intervals with n . This can be seen for all fields of the Schwarzschild and extremal Reissner-Nordström BH, and additionally for the spin-1 aQNFs of the Schwarzschild dS BH, for the spin-1/2 aQNFs in the Schwarzschild and Reissner-Nordström BHs, and for the spin-3/2 aQNFs of the Schwarzschild dS BH.

While a physical interpretation of our results is not immediately clear, the absence of a constant proportional to the natural logarithm of an integer in most cases weakens the already tenuous connection between aQNFs and a quantum spectrum of BHs. The BH area quantisation extracted from the real part of the aQNF is therefore not an intrinsic property of the BH [29]. As suggested in section V of Ref. [4], if a link between aQNFs and quantum gravity exists, it is likely to be more subtle than Hod's conjecture would imply. However, as argued by Maggiore [29], it may be that the underlying principles of Hod's conjecture were not well applied to begin with: Bohr's correspondence principle, for example, is valid for $n \leftrightarrow n'$ transitions where $n, n' \gg 1$; Hod considered instead the excitation of a BH from

the ground state. Through the use of $(\omega_0)_n$ (as defined in section I) for the real frequency in the transition $n \rightarrow n - 1$, Maggiore recovered Bekenstein’s original Schwarzschild BH area irrespective of the spin of the field. As such, the consistent behaviour of $(\omega_0)_n$ within the large- n limit led Maggiore to an BH area quantisation intrinsic to the Schwarzschild BH [29]. It would be interesting to explore whether this can be extended beyond the Schwarzschild case.

Despite the interest in aQNFs, there are relatively few examples in the literature of aQNF computations, both analytical and numerical. Consequently, there are few aQNF results available within the literature. This work then serves as a collection of known results and a point of reference against which future studies may compare. There is a pronounced scarcity in numerical checks for aQNF results: beyond Leaver’s continued fraction method (which is limited in the case of extremal Reissner-Nordström BHs, as discussed in section II C 2), few numerical attempts have been applied to aQNFs. The debate surrounding the aQNF expression for the Reissner-Nordström and the unusual Dirac result obtained in this work emphasise this need for further study into numerical validation for aQNFs. In this respect, our analytical results may help guide the development of numerical techniques to approach the highly damped QNFs.

Future research into the large overtone limit should seek out a justification for the observations made within this paper, particularly on the consistency of the Dirac results across various BH spacetimes. An investigation into the Rarita-Schwinger aQNFs is also necessary, to determine why the spin-3/2 aQNF behaviour resembles gravitational perturbations in certain Reissner-Nordström BH contexts but Dirac perturbations in the Schwarzschild and Schwarzschild dS BH spacetimes. That this behaviour for the nonTT spin-3/2 modes holds only under the $\mu \gg \vartheta\kappa$ limit should also be assessed. The possible SUSY considerations that arise for these aQNFs of spin-3/2 and spin-2 in the extremal Reissner-Nordström context also require further considerations. Here, the need for aQNF expressions corresponding to perturbing electromagnetic fields within Reissner-Nordström BH spacetimes becomes especially apparent.

Furthermore, an extension of the aQNF investigation conducted here focused on dimensionality, in the style of Ref. [38], would verify explicitly the claims in the literature regarding the generalisability of the $d = 6$ monodromy results reviewed in subsection II C. While we are aware of the anomalous behaviour of 5D BHs, we might infer from Figs. 2, 3, and 4

that odd dimensions may require individual analysis. This is particularly important for BH spacetimes inclusive of the cosmological constant. Finally, whether the monodromy technique, or some variant thereof, may be applied to rotating BH spacetimes is an interesting open question.

ACKNOWLEDGMENTS

CHC is supported in part by the Naresuan University Research Fund R2565C012. HTC is supported in part by the Ministry of Science and Technology, Taiwan, under the Grants No. MOST108-2112-M-032-002 and MOST109-2112-M-032-007. ASC is supported in part by the National Research Foundation (NRF) of South Africa. AC is supported by a Campus France Scholarship, and the NRF and Department of Science and Innovation through the SA-CERN programme. The authors would like to thank the anonymous reviewers for their thorough and insightful reports.

-
- [1] H.-P. Nollert, *Class. Quant. Grav.* **16**, R159 (1999).
 - [2] K. D. Kokkotas and B. G. Schmidt, *Living Rev. Rel.* **2**, 2 (1999), [arXiv:gr-qc/9909058](#).
 - [3] E. Berti, V. Cardoso, and A. O. Starinets, *Class. Quant. Grav.* **26**, 163001 (2009), [arXiv:0905.2975 \[gr-qc\]](#).
 - [4] R. A. Konoplya and A. Zhidenko, *Rev. Mod. Phys.* **83**, 793 (2011), [arXiv:1102.4014 \[gr-qc\]](#).
 - [5] E. W. Leaver, *Proc. Roy. Soc. Lond. A* **402**, 285 (1985).
 - [6] E. W. Leaver, *J. Math. Phys* **27**, 1238 (1986).
 - [7] E. W. Leaver, *Phys. Rev. D* **34**, 384 (1986).
 - [8] V. Cardoso and J. P. S. Lemos, *Phys. Rev. D* **64**, 084017 (2001).
 - [9] V. Cardoso, J. P. S. Lemos, and S. Yoshida, *Phys. Rev. D* **69**, 044004 (2004), [arXiv:gr-qc/0309112](#).
 - [10] E. Berti and K. D. Kokkotas, *Phys. Rev. D* **68**, 044027 (2003), [arXiv:hep-th/0303029](#).
 - [11] N. Andersson and S. Linnæus, *Phys. Rev. D* **46**, 4179 (1992).
 - [12] N. Andersson, *Class. Quant. Gravity* **10**, L61 (1993).
 - [13] N. Andersson and C. J. Howls, *Class. Quant. Grav.* **21**, 1623 (2004), [arXiv:gr-qc/0307020](#).

- [14] L. Motl, *Adv. Theor. Math. Phys.* **6**, 1135 (2003), arXiv:gr-qc/0212096.
- [15] L. Motl and A. Neitzke, *Adv. Theor. Math. Phys.* **7**, 307 (2003), arXiv:hep-th/0301173.
- [16] J. Natário and R. Schiappa, *Adv. Theor. Math. Phys.* **8**, 1001 (2004), arXiv:hep-th/0411267.
- [17] S. Das and S. Shankaranarayanan, *Class. Quant. Grav.* **22**, L7 (2005), arXiv:hep-th/0410209.
- [18] A. Ghosh, S. Shankaranarayanan, and S. Das, *Class. Quant. Grav.* **23**, 1851 (2006), arXiv:hep-th/0510186.
- [19] D. Birmingham, *Phys. Lett. B* **569**, 199 (2003).
- [20] R. G. Daghigh and G. Kunstatter, *Class. Quant. Grav.* **22**, 4113 (2005), arXiv:gr-qc/0505044.
- [21] R. G. Daghigh and G. Kunstatter, *Can. J. Phys.* **84**, 473 (2006), arXiv:gr-qc/0507019.
- [22] R. G. Daghigh, G. Kunstatter, D. Ostapchuk, and V. Bagnulo, *Class. Quant. Grav.* **23**, 5101 (2006), arXiv:gr-qc/0604073.
- [23] R. G. Daghigh and M. D. Green, *Class. Quant. Grav.* **25**, 055001 (2008), arXiv:0708.1333 [gr-qc].
- [24] J. Babb, R. Daghigh, and G. Kunstatter, *Phys. Rev. D* **84**, 084031 (2011), arXiv:1106.4357 [gr-qc].
- [25] H. T. Cho, *Phys. Rev. D* **73**, 024019 (2006), arXiv:gr-qc/0512052.
- [26] A. López-Ortega, *Gen. Rel. Grav.* **38**, 1747 (2006), arXiv:gr-qc/0605034.
- [27] M. Casals and A. C. Ottewill, *Phys. Rev. D* **97**, 024048 (2018), arXiv:1606.03423 [gr-qc].
- [28] O. Dreyer, *Phys. Rev. Lett.* **90**, 081301 (2003), arXiv:gr-qc/0211076.
- [29] M. Maggiore, *Phys. Rev. Lett.* **100**, 141301 (2008), arXiv:0711.3145 [gr-qc].
- [30] J. Skakala and M. Visser, *Phys. Rev. D* **81**, 125023 (2010), arXiv:1007.4039 [gr-qc].
- [31] S. Hod, *Phys. Rev. Lett.* **81**, 4293 (1998), arXiv:gr-qc/9812002.
- [32] J. D. Bekenstein, *Lett. Nuovo Cim.* **4**, 737 (1972).
- [33] V. F. Mukhanov, *JETP Lett.* **44**, 63 (1986).
- [34] J. D. Bekenstein and V. F. Mukhanov, *Phys. Lett. B* **360**, 7 (1995), arXiv:gr-qc/9505012.
- [35] H.-P. Nollert, *Phys. Rev. D* **47**, 5253 (1993).
- [36] V. Cardoso and J. P. S. Lemos, *Phys. Rev. D* **67**, 084020 (2003).
- [37] V. Cardoso, J. Natario, and R. Schiappa, *J. Math. Phys.* **45**, 4698 (2004), arXiv:hep-th/0403132.
- [38] R. G. Daghigh and M. D. Green, *Class. Quant. Grav.* **26**, 125017 (2009), arXiv:0808.1596 [gr-qc].

- [39] P. Arnold and P. Szepietowski, *Phys. Rev. D* **88**, 086002 (2013), [arXiv:1308.0341 \[hep-th\]](#).
- [40] P. Arnold, P. Szepietowski, and D. Vaman, *Phys. Rev. D* **89**, 046001 (2014), [arXiv:1311.6409 \[hep-th\]](#).
- [41] A. J. M. Medved, *Class. Quant. Grav.* **25**, 205014 (2008), [arXiv:0804.4346 \[gr-qc\]](#).
- [42] R. G. Daghigh, M. D. Green, J. C. Morey, and G. Kunstatter, *Phys. Rev. D* **102**, 104040 (2020), [arXiv:2009.02367 \[gr-qc\]](#).
- [43] H. Kodama and A. Ishibashi, *Prog. Theor. Phys.* **110**, 701 (2003), [arXiv:hep-th/0305147](#).
- [44] A. Ishibashi and H. Kodama, *Prog. Theor. Phys.* **110**, 901 (2003), [arXiv:hep-th/0305185](#).
- [45] H. Kodama and A. Ishibashi, *Prog. Theor. Phys.* **111**, 29 (2004), [arXiv:hep-th/0308128](#).
- [46] A. Ishibashi and H. Kodama, *Prog. Theor. Phys. Suppl.* **189**, 165 (2011), [arXiv:1103.6148 \[hep-th\]](#).
- [47] T. Regge and J. A. Wheeler, *Phys. Rev.* **108**, 1063 (1957).
- [48] F. J. Zerilli, *Phys. Rev. D* **9**, 860 (1974).
- [49] V. Moncrief, *Phys. Rev. D* **9**, 2707 (1974).
- [50] V. Moncrief, *Phys. Rev. D* **10**, 1057 (1974).
- [51] V. Moncrief, *Phys. Rev. D* **12**, 1526 (1975).
- [52] Y. Decanini, A. Folacci, and B. Raffaelli, *Phys. Rev. D* **84**, 084035 (2011), [arXiv:1108.5076 \[gr-qc\]](#).
- [53] C.-H. Chen, H.-T. Cho, and A. S. Cornell, *Chin. J. Phys.* **67**, 646 (2020), [arXiv:2004.05806 \[gr-qc\]](#).
- [54] C.-H. Chen, H.-T. Cho, A. Chrysostomou, and A. S. Cornell, (2021), [arXiv:2103.07777 \[gr-qc\]](#).
- [55] R. G. Daghigh and M. D. Green, *Phys. Rev. D* **85**, 127501 (2012), [arXiv:1112.5397 \[gr-qc\]](#).
- [56] G. C. Wick, *Phys. Rev.* **96**, 1124 (1954).
- [57] M. Abramowitz and I. A. Stegun, Handbook of Mathematical Functions, 6th ed. (U.S. Government Printing Office, Washington D.C., 1964).
- [58] E. Berti and K. D. Kokkotas, *Phys. Rev. D* **67**, 064020 (2003), [arXiv:gr-qc/0301052](#).
- [59] E. Berti, *Conf. Proc. C* **0405132**, 145 (2004), [arXiv:gr-qc/0411025](#).
- [60] H. Onozawa, T. Mishima, T. Okamura, and H. Ishihara, *Phys. Rev. D* **53**, 7033 (1996), [arXiv:gr-qc/9603021](#).
- [61] J. D. Bekenstein, *Lett. Nuovo Cim.* **11**, 467 (1974).

- [62] H. Onozawa, T. Okamura, T. Mishima, and H. Ishihara, *Phys. Rev. D* **55**, 1 (1997).
- [63] R. Kallosh, J. Rahmfeld, and W. K. Wong, *Phys. Rev. D* **57**, 1063 (1998), [arXiv:hep-th/9706048](#).
- [64] F. J. Zerilli, *Phys. Rev. D* **2**, 2141 (1970).
- [65] L. C. B. Crispino, A. Higuchi, and G. E. A. Matsas, *Phys. Rev. D* **63**, 124008 (2001), [Erratum: *Phys.Rev.D* 80, 029906 (2009)].
- [66] F. Cooper, A. Khare, and U. Sukhatme, *Physics Reports* **251**, 267 (1995).
- [67] C. H. Chen, H. T. Cho, A. S. Cornell, G. Harmsen, and W. Naylor, *Chin. J. Phys.* **53**, 110101 (2015), [arXiv:1504.02579 \[gr-qc\]](#).
- [68] C. H. Chen, H. T. Cho, A. S. Cornell, and G. Harmsen, *Phys. Rev. D* **94**, 044052 (2016), [arXiv:1605.05263 \[gr-qc\]](#).
- [69] C. H. Chen, H. T. Cho, A. S. Cornell, G. Harmsen, and X. Ngcobo, *Phys. Rev. D* **97**, 024038 (2018), [arXiv:1710.08024 \[gr-qc\]](#).
- [70] C.-H. Chen, H.-T. Cho, A. S. Cornell, and G. E. Harmsen, *Phys. Rev. D* **100**, 104018 (2019), [arXiv:1907.11856 \[gr-qc\]](#).
- [71] H. T. Cho, A. S. Cornell, J. Doukas, and W. Naylor, *Phys. Rev. D* **75**, 104005 (2007), [arXiv:hep-th/0701193](#).
- [72] S. K. Chakrabarti, *Eur. Phys. J. C* **61**, 477 (2009), [arXiv:0809.1004 \[gr-qc\]](#).
- [73] R. Kallosh, A. D. Linde, T. Ortin, A. W. Peet, and A. Van Proeyen, *Phys. Rev. D* **46**, 5278 (1992), [arXiv:hep-th/9205027](#).
- [74] R. Kallosh, *Phys. Lett. B* **282**, 80 (1992), [arXiv:hep-th/9201029](#).
- [75] G. W. Gibbons and C. M. Hull, *Phys. Lett. B* **109**, 190 (1982).
- [76] J. B. Hartle and S. W. Hawking, *Commun. Math. Phys.* **26**, 87 (1972).